

FAM83F regulates canonical Wnt signalling through an interaction with CK1 α

Karen Dunbar¹, Rebecca A. Jones², Kevin Dingwell², Thomas J. Macartney¹, James C. Smith² and Gopal P. Sapkota^{1*}

¹ MRC Protein Phosphorylation and Ubiquitylation Unit, School of Life Sciences, University of Dundee, Sir James Black Centre, Dow Street, Dundee, DD1 5EH, United Kingdom.

² The Francis Crick Institute, 1 Midland Road, London, NW1 1AT, United Kingdom.

*Correspondence and requests for materials should be addressed to:
g.sapkota@dundee.ac.uk

Running title:

FAM83F-CK1 α complex mediates Wnt signalling

Keywords:

Colorectal cancer, *Xenopus* axis duplication, farnesylation, plasma membrane

ABSTRACT

The function of the FAM83F protein, like the functions of many members of the FAM83 family, is poorly understood. Here we show that injection of Fam83f mRNA into *Xenopus* embryos causes axis duplication, a phenotype indicative of enhanced Wnt signalling. Consistent with this, overexpression of FAM83F activates Wnt signalling, whilst ablation of FAM83F from human colorectal cancer (CRC) cells attenuates it. We demonstrate that FAM83F is farnesylated and interacts and co-localises with CK1 α at the plasma membrane. This interaction with CK1 α is essential for FAM83F to activate Wnt signalling, and FAM83F mutants that do not interact with CK1 α fail to induce axis duplication in *Xenopus* embryos and to activate Wnt signalling in cells. FAM83F acts upstream of the β -catenin destruction complex, because the attenuation of Wnt signalling caused by loss of FAM83F can be rescued by GSK-3 inhibition. Introduction of a farnesyl-deficient mutant mis-localises the FAM83F-CK1 α complex to the nucleus and significantly attenuates Wnt signalling, indicating that FAM83F exerts its effects on Wnt signalling at the plasma membrane.

INTRODUCTION

FAM83F belongs to the FAM83 family of proteins, which is characterised by a conserved N-terminal DUF1669 domain. We have recently shown that the DUF1669 domain mediates interaction with the α , δ or ϵ isoforms of the CK1 family of Ser/Thr protein kinases (1). The FAM83 proteins direct the CK1 isoforms with which they interact to distinct subcellular compartments, thereby potentially regulating their substrate pools (1). All FAM83 proteins interact with CK1 α , albeit with varying affinity, while FAM83A, B, E and H also interact with CK1 δ and ϵ isoforms (1). CK1 α , δ and ϵ isoforms have been implicated in numerous cellular processes including Wnt signalling, mitosis, circadian rhythm and DNA damage responses (2-5).

There is now increasing evidence that FAM83 proteins regulate the diverse biological roles of CK1 isoforms. For example, FAM83G (a.k.a. PAWS1) regulates canonical Wnt signalling downstream of the β -catenin destruction complex through association with CK1 α (6). Interestingly, two mutations within the DUF1669 domain of the *FAM83G* gene that cause palmoplantar keratoderma result in the loss of FAM83G-CK1 α interaction and attenuation of Wnt signalling (7). FAM83D directs CK1 α to the mitotic spindle to ensure proper spindle alignment and timely exit from mitosis (8), and FAM83H mutations that cause amelogenesis imperfecta retain interaction with CK1 isoforms but are mis-localised in cells (9, 10). However, the biological and biochemical roles of FAM83F are poorly understood. High levels of FAM83F protein have been linked to oncogenesis in glioma (11), lung cancer (12), oesophageal cancer (13) and thyroid cancer (14) yet the underlying mechanisms remain unknown. Sequence alignment of the conserved DUF1669 domain reveals that FAM83F most resembles FAM83G and is the only other FAM83 protein to induce Wnt reporter activity in an overexpression assay (Sup. Fig. 1). We therefore sought to explore whether FAM83F is also involved in regulating canonical Wnt signalling.

Wnt signalling plays important roles in embryogenesis and cell proliferation as well as in stem cell and adult tissue homeostasis (15). The key effector of the canonical Wnt signalling pathway is β -catenin. Under basal conditions, most β -catenin protein is located at the adherens junctions, while cytoplasmic β -catenin levels are kept in check by the β -catenin destruction complex. The destruction complex is composed principally of two scaffold proteins, Axin and Adenomatous polyposis coli (APC), and two protein kinases, glycogen synthase kinase-3 β (GSK-3 β) and casein kinase 1 α (CK1 α). Phosphorylation of β -catenin at S45 by CK1 α primes β -catenin for GSK-3 β mediated sequential phosphorylation at T41, S37 and S33, which allows the β -transducin repeat-containing protein (β -Trcp) to ubiquitylate β -catenin and facilitate its degradation through the proteasome (16). Upon binding Wnt

ligands, the Wnt receptor Frizzled and co-receptor LRP6 recruit Dishevelled and the β -catenin destruction complex to the plasma membrane. This complex, termed the Wnt signalosome, in turn becomes internalised in multivesicular bodies, thus sparing the degradation of cytoplasmic β -catenin (17). The resultant stabilised β -catenin then translocates to the nucleus, where it binds to its co-transcriptional factor, T-cell factor (TCF), and triggers the transcription of Wnt target genes, such as *Axin2*, *C-myc* and *Cyclin D1* (18). Aberrant Wnt signalling is a common feature in various cancers, particularly those of gastrointestinal origin including a vast majority of colorectal cancers (CRC) (19).

In this study we explore the role of FAM83F in driving Wnt signalling in *Xenopus* embryos and tissue culture cells, including CRC cells.

RESULTS

FAM83F induces axis duplication in *Xenopus* embryos through an interaction with CK1 α .

The activation of the canonical Wnt signalling pathway by ectopic expression of Wnt ligands and mediators in early *Xenopus* embryos causes axis duplication (20). Previously, we showed that injection of *Xenopus* embryos with *FAM83G* mRNA into a ventral blastomere at the four-cell stage induced secondary axis formation (6). The expression of mRNA in early *Xenopus* embryos is thus an efficient method for screening potential regulators of canonical Wnt signalling. Upon injection of axis-inducing mRNA, four possible axial phenotypes can result, including complete secondary axes, partial secondary axes, dorsalised embryos and those resembling wild-type (Fig. 1A). To test the impact of FAM83F on *Xenopus* embryos, 500 pg of mRNA encoding HA-tagged zebrafish *Fam83fa*, which closely resembles FAM83F in human and other species and was the only construct available at the time, was injected into a single ventral blastomere at the four-cell stage. Embryos were maintained until approximately stage 35, at which point we counted the embryos displaying each class of axial phenotype. HA-*Fam83fa* induced secondary axes in >60% of the *Xenopus* embryos (Fig. 1B&C). A second zebrafish orthologue of FAM83F, *Fam83fb*, did not induce axis duplication (Fig. 1B), despite being more robustly expressed than *Fam83fa*, as shown by Western blot (Fig. 1C).

FAM83F interacts selectively with CK1 α through its conserved DUF1669 domain and mutating the phenylalanine residues from a conserved F-X-X-X-F motif to alanine abolishes this interaction (1). In zebrafish *Fam83fa*, these two phenylalanine residues map at amino acid positions 275 and 279. Mutation of either F275 or F279 to an alanine prevented the

induction of a secondary axis (Fig. 1D), as did the double mutant, Fam83fa^{F275/279A}, despite all proteins being expressed, as shown by Western blot (Fig. 1E). This indicates that Fam83fa-CK1 α binding is required for Fam83fa to induce axis duplication in *Xenopus* embryos. When we tested Fam83fa fragments with deletions at the C-terminus for their ability to induce axis duplication, both full-length *fam83fa* mRNA (*HA-fam83fa*^{1-555aa}) and the DUF1669 domain fragment (*HA-fam83fa*^{1-300aa}) induced secondary axes robustly (Sup. Fig. 2A&B). Interestingly, the C-terminal deletions *HA-fam83fa*^{1-500aa}, *HA-fam83fa*^{1-400aa} and *HA-fam83fa*^{1-355aa} induced secondary axes poorly, indicating that loss of the C-terminal portion of the protein affects Fam83fa structure or function.

Human FAM83F contains a protein prenylation motif, a conserved CAAX box sequence at the C-terminus in which the Cys residue is modified through an addition of either a geranylgeranyl or a farnesyl moiety (21). When FAM83F that has been overexpressed in HEK293 cells was isolated, cleaved with trypsin and subjected to mass-spectrometry, we identified tryptic peptides found to be farnesylated at Cys497 (Sup. Fig. 3). Farnesylation, a posttranslational modification, involves the addition of a 15-carbon farnesyl group to a C-terminal cysteine residue by farnesyltransferase; this plays a role in the regulation of protein-membrane interactions and in signal transduction circuits (22). Zebrafish Fam83fa, which possesses the CIQS sequence at its C-terminus, is also predicted to be farnesylated (23). Mutation in the human protein of the CAAX-box invariant cysteine to an alanine, creating FAM83F^{C497A}, prevents farnesylation but injection of mRNA encoding this mutated protein induced secondary axis formation in *Xenopus* embryos in a similar manner to that of wild-type *FAM83F* (Sup. Fig. 2C). This indicates that farnesylation of the C-terminus of FAM83F is not required for its ability to activate canonical Wnt signalling in the *Xenopus* assays.

FAM83F-CK1 α interaction is required for FAM83F membrane localisation and canonical Wnt signalling effects.

Initial investigations of FAM83F biology were performed in the U2OS Flp-In T-Rex (Flp/Trx) cell line, which allows doxycycline inducible gene expression of stably integrated proteins of interest. Stable cell lines were generated to express GFP only, GFP-FAM83A, GFP-FAM83F, GFP-FAM83F^{C497A}, GFP-FAM83F^{D250A} and GFP-FAM83F^{F284/288A}. Immunoprecipitation of GFP confirmed that GFP-FAM83F interacts with CK1 α but no interaction was detected with GFP only or with GFP-FAM83A (Fig. 2A). GFP-FAM83F^{F284/288A} does not interact with CK1 α , whilst the interaction between GFP-FAM83F^{D250A} and CK1 α is severely reduced compared with wild type GFP-FAM83F. The farnesyl-deficient mutant, GFP-FAM83F^{C497A}, still maintains an interaction with CK1 α (Fig. 2A).

Fluorescence microscopy showed that GFP-FAM83F is present predominately at the plasma membrane in U2OS Flp/Trx cells, with some nuclear staining also observed (Fig. 2B). The farnesyl-deficient mutant GFP-FAM83F^{C497A} was detectable only in the nucleus, suggesting that farnesylation of FAM83F directs its localisation to the plasma membrane. Interestingly, the two CK1 α -binding deficient mutants, GFP-FAM83F^{D250A} and GFP-FAM83F^{F284/288A}, exhibited cytoplasmic and peri-nuclear localisation away from the plasma membrane and the nucleus. This suggests that the membrane and nuclear localisation of FAM83F is facilitated by its association with CK1 α . Co-staining with an anti-CK1 α antibody revealed overlapping localisation with GFP-FAM83F and GFP-FAM83F^{C497A}, but not with GFP-FAM83F^{D250A} and GFP-FAM83F^{F284/288A} (Fig. 2B).

Canonical Wnt signalling activity can be measured using a dual luciferase reporter assay in which cells are transfected with a plasmid containing either wild-type TCF binding sites (TOPflash) or mutant TCF binding sites (FOPflash) upstream of a luciferase reporter (24). T-cell factor (TCF) is a co-transcriptional activator of β -catenin, so an increase in canonical Wnt signalling activity causes β -catenin to bind to TCF and induce luciferase expression and hence activity (25). Overexpression of GFP-FAM83F and GFP-FAM83F^{C497A} significantly increased luciferase reporter activity in cells treated with control L- conditioned media compared with GFP controls (Fig. 2C). In contrast, overexpression of the CK1 α -binding deficient mutants GFP-FAM83F^{D250A} and GFP-FAM83F^{F284/288A} did not increase luciferase activity under these conditions. Following addition of Wnt3A-conditioned medium, GFP-FAM83F and GFP-FAM83F^{C497A} cell lines had significantly increased luciferase activity when compared with Wnt3A-treated GFP controls (Fig. 2C). Wnt3A-induced luciferase reporter activity in cells expressing the CK1 α -binding deficient mutants GFP-FAM83F^{D250A} and GFP-FAM83F^{F284/288A} was substantially lower than in cells expressing GFP-FAM83F and GFP-FAM83F^{C497A} (Fig. 2C). This suggests that FAM83F-induced Wnt reporter activity is mediated through its association with CK1 α .

Endogenous FAM83F localises to the plasma membrane and interacts with CK1 α .

To facilitate the study of endogenous FAM83F protein we screened multiple tissues and cell lines to identify cell lines with detectable levels of endogenous FAM83F protein. Tissue-specific expression of FAM83F from mouse tissue extracts revealed that FAM83F protein was detected in spleen, lung and gastrointestinal tissues, with the highest levels of FAM83F protein detected in the stomach, small intestine, large intestine and intestinal crypts (Fig. 3A). Similar assessment of a panel of routinely studied cell lines showed that FAM83F protein was detected in extracts from the mammary adenocarcinoma cell line MDA-MB-468,

and the colorectal cancer cell line HCT116, but was undetectable in many other cell lines (Sup. Fig.4). Separately, we detected FAM83F protein in extracts from HaCaT keratinocytes as well as DLD-1 colorectal cells (Fig. 3A&B). Based on the abundance of FAM83F protein observed in gastrointestinal tissue extracts and colorectal cells, we proceeded with two colorectal cancer cell lines, HCT116 and DLD-1, for further investigation into the role of endogenous FAM83F in canonical Wnt signalling. By using CRISPR/Cas9 technology, we generated FAM83F knockout (FAM83F^{-/-}) HCT116 (clones 1 and 2) and DLD-1 cells and also knocked in a GFP tag N-terminal to the *FAM83F* gene homozygously in both cell lines (HCT116^{GFP/GFP}FAM83F and DLD-1^{GFP/GFP}FAM83F) (Fig. 3B). Both knockouts and GFP-knockins were verified by DNA sequencing and Western blotting (Fig. 3B and Sup. Fig. 5).

GFP-FAM83F immunoprecipitates (IPs) from HCT116^{GFP/GFP}FAM83F and DLD-1^{GFP/GFP}FAM83F cell extracts but not from wild-type cells co-precipitated endogenous CK1 α , but not CK1 δ or CK1 ϵ (Fig. 3C). Similarly, endogenous CK1 α IPs co-precipitated FAM83F from wild-type HCT116 and DLD-1 cell extracts but not from HCT116 FAM83F^{-/-} (cl.1) and DLD-1 FAM83F^{-/-} cell extracts (Fig. 3D). The interaction between CK1 α and FAM83G was unaffected by FAM83F knockout, because CK1 α IPs co-precipitated FAM83G from all cell extracts (Fig. 3D). Endogenously driven GFP-FAM83F in HCT116^{GFP/GFP}FAM83F knockin cells localised predominately to the plasma membrane, as revealed by anti-GFP immunofluorescence (Fig. 3E). Under these conditions, endogenous CK1 α immunostaining exhibited a diffuse pan-cellular staining, which limited the detection of plasma membrane-specific co-localisation with GFP-FAM83F. Immunofluorescence using a FAM83F antibody in HCT116 wild-type cells confirmed the plasma membrane localisation of endogenous FAM83F, which co-localised with β -catenin, a marker of the adherens junctions (Fig.3F). The specificity of anti-FAM83F staining was demonstrated using HaCaT wild-type and FAM83F^{-/-} cell lines (Sup. Fig. 6).

Knockout of FAM83F reduces canonical Wnt signalling in colorectal cancer cells.

Constitutively active Wnt signalling is a hallmark of many colorectal cancers (CRCs) (19). Mutations in the *APC* gene, which encodes a central component of the β -catenin destruction complex and facilitates the destruction of free cytoplasmic β -catenin, are among the most common in CRCs (26). DLD-1 cells express APC truncated at residue 1417, whilst HCT116 cells have a heterozygous mutation of β -catenin at S45, which prevents β -catenin from being phosphorylated and then ubiquitinated and degraded (27, 28). Thus, constitutive activation of Wnt signalling in HCT116 and DLD-1 cells occurs through perturbations at different stages of the pathway, and the responses to Wnt3A-ligand stimulation are also likely to differ. Canonical Wnt signalling activity can be measured by the transcript expression of Wnt target

genes such as *Axin2* (18) as demonstrated by the >2-fold increase in *Axin2* mRNA expression following the addition of Wnt3A-CM to wild-type HCT116 cells (Fig. 4A). In both HCT116 FAM83F^{-/-} clones, the Wnt3A-induced increase in *Axin2* mRNA abundance was significantly reduced compared with wild-type HCT116 cells. Neither wild-type DLD-1 cells nor DLD-1 FAM83F^{-/-} cells were responsive to treatment with Wnt3A-CM, but DLD-1 FAM83F^{-/-} cells had a slight but significant reduction in basal *Axin2* mRNA abundance. In addition to the two colorectal cancer cell lines, we generated a FAM83F knockout in the osteosarcoma cell line U2OS (Sup. Fig. 7A). Endogenous FAM83F protein abundance is low in U2OS cells, with detection only possible after immunoprecipitation with an anti-FAM83F antibody. Canonical Wnt activity was determined using the dual luciferase assay (Sup. Fig. 7B) and the endogenous Wnt target gene *Axin2* (Sup. Fig. 7C). U2OS wild-type and U2OS FAM83F^{-/-} cells respond to Wnt3A stimulus with increased luciferase activity and *Axin2* mRNA abundance respectively, but the extent of both responses was significantly reduced in U2OS FAM83F^{-/-} cells compared to U2OS wild-type cells (Sup. Fig. 7B&C).

We next sought to determine whether the FAM83F-CK1 α interaction is affected by Wnt3a stimulation. CK1 α IPs co-precipitated endogenous FAM83F from wild-type HCT116 and DLD-1 cell extracts but not from HCT116-FAM83F^{-/-} (cl.1) and DLD-1-FAM83F^{-/-} cell extracts regardless of stimulation with L-CM or Wnt3A-CM for 6 h (Fig. 4B). We also analysed the components of the canonical Wnt3A signalling pathway in these cells upon stimulation with Wnt3A-CM (Fig. 4C). A slight reduction in phospho- β -catenin (S45) was detected in wild type and FAM83F^{-/-} HCT116 cells following addition of Wnt3A-CM compared to L-CM controls, indicating activation of the signalling pathway. The levels of phospho-LRP6 (S1490), total LRP6, phospho- β -catenin (S33/S37/T41), active β -catenin and total β -catenin were similar in HCT116 wild-type, HCT116 FAM83F^{-/-} (cl.1) and HCT116 FAM83F^{-/-} (cl.2) cells, regardless of Wnt3A stimulation (Fig. 4C). Although there was a slight increase in LRP6 levels in DLD-1-FAM83F^{-/-} cells relative to wild-type DLD-1 cells, no consistent changes in the abundance of any other Wnt signalling pathway proteins or phospho-proteins was evident between wild-type and FAM83F knockout DLD-1 cells, regardless of Wnt3A stimulation.

FAM83F acts upstream of the β -catenin destruction complex.

We sought to investigate where within the canonical Wnt/ β -catenin signalling pathway FAM83F was acting. If the inhibition of Wnt signalling upon FAM83F loss can be restored by GSK-3 inhibitors, which prevent the phosphorylation and subsequent ubiquitin-mediated proteasomal degradation of β -catenin, this would imply that FAM83F acts upstream of the β -catenin destruction complex. As previously noted, Wnt3A-induced *Axin2* mRNA abundance

was lower in HCT116 FAM83F^{-/-} cells compared to wild-type HCT116 cells (Fig. 4A). However, treatment of wild-type HCT116 and HCT116 FAM83F^{-/-} cells with 5 μM CHIR99021, a selective GSK-3 inhibitor, enhanced *Axin2* mRNA abundance to a similar extent in both cell lines regardless of Wnt3A stimulation (Fig. 5A). In a similar assay, when U2OS wild-type and U2OS FAM83F^{-/-} cells were treated with 5 μM of CHIR99021, *Axin2* mRNA abundance increased to a similar extent in both cell lines regardless of Wnt3A stimulation (Sup. Fig. 7C). These observations indicate that FAM83F acts to modulate Wnt signalling upstream of the β-catenin destruction complex.

Given the plasma membrane localisation of FAM83F, as detected by immunofluorescence (Fig. 2B and Fig. 3E&F), we hypothesised that FAM83F may influence canonical Wnt signalling at the membrane. Wild-type HCT116, HCT116 FAM83F^{-/-} (cl.1) and HCT116 FAM83F^{-/-} (cl.2) cells were separated into cytoplasmic, nuclear and membrane fractions (Fig. 5B). In wild-type HCT116 cells, FAM83F was detected predominately in the membrane fraction with a small proportion in the nuclear fraction, whilst CK1α was detected in all three fractions: cytoplasmic, nuclear and membrane (Fig. 5C). Interestingly, CK1α protein abundance in the membrane fraction was significantly reduced in both HCT116 FAM83F^{-/-} (cl.1) and HCT116 FAM83F^{-/-} (cl.2) cells compared to HCT116 wild-type cells (Fig. 5C). A similar result was observed using DLD-1 FAM83F^{-/-} and DLD-1 wild-type cells (Fig. 5D&E). These results suggest that FAM83F directs CK1α to the plasma membrane.

Membranous localisation of FAM83F is required for FAM83F's role in canonical Wnt signalling.

To investigate the importance of membrane bound FAM83F in canonical Wnt signalling, we introduced a point mutation into the farnesylation motif of FAM83F, which should prevent membrane anchorage of FAM83F. Using CRISPR/Cas9, we sought to introduce a C497A mutation into the *FAM83F* gene in HCT116 cells. Unfortunately, we were only able to isolate a single heterozygous clone, HCT116 FAM83F^{WT/C497A}. Nonetheless, when we separated wild-type HCT116, HCT116 FAM83F^{WT/C497A} and HCT116 FAM83F^{-/-} (cl.2) cell extracts into cytoplasmic, nuclear and membrane fractions, FAM83F protein was detected predominately in the nuclear fraction in HCT116 FAM83F^{WT/C497A} cells, with a smaller proportion at the membrane, in a manner resembling the localisation detected with overexpression of GFP-FAM83F^{C497A} (Fig. 6A and Fig. 2B). Quantification of membrane localised FAM83F and CK1α protein abundance showed a significant reduction in both proteins in HCT116 FAM83F^{WT/C497A} cells compared to wild-type HCT116 cells, while a further reduction was noted in HCT116 FAM83F^{-/-} cells (Fig. 6B). CK1α IPs from wild-type HCT116 and HCT116 FAM83F^{WT/C497A} cell extracts co-precipitated FAM83F but not from HCT116 FAM83F^{-/-} cells

Fig. 6C), confirming that farnesylation of FAM83F does not affect CK1 α binding. Wnt3A-induced expression of *Axin2* mRNA was slightly but significantly reduced in HCT116 FAM83F^{WT/C497A} cells compared to wild-type HCT116 cells (Fig. 6D), indicating that membrane bound FAM83F is required for canonical Wnt signalling.

DISCUSSION

We know little about the function of FAM83F. In this study, we show that FAM83F mediates the canonical Wnt/ β -catenin signalling pathway both in developing *Xenopus* embryos and in human cancer cells. We show that FAM83F is localised at the plasma membrane through farnesylation and directs CK1 α to the plasma membrane. The FAM83F-CK1 α complex appears to act upstream of the β -catenin destruction complex and we show that the interaction between FAM83F and CK1 α and their membrane localisation is essential for driving Wnt signalling.

CK1 isoforms have been implicated in both positive and negative regulation of Wnt/ β -catenin signalling (3). This suggests that the activity of CK1 isoforms is tightly regulated in a spatiotemporal manner. As key regulators of the CK1 isoforms, it is highly likely that the FAM83 proteins play a role. Any perturbation of the homeostatic balance of endogenous CK1 pools in cells, caused for example by overexpression of interacting proteins, is thus likely to disrupt coordinated roles of CK1 isoforms in Wnt signalling. This could explain the apparent contradictory observations we made when the overexpression of FAM83F^{C497A} in *Xenopus* embryos and in cells caused an increase in canonical Wnt signalling, while the replacement of an allele of endogenous FAM83F with FAM83F^{C497A} attenuated Wnt signalling. Expressing high levels of FAM83F^{C497A} protein, which redirects much of the endogenous CK1 α protein to the nucleus, potentially causes a reduction in the cytoplasmic pool of CK1 α , thus removing inhibitory CK1 α from the β -catenin destruction complex and thereby activating the canonical Wnt signalling pathway.

We have shown that FAM83F and FAM83G/PAWS1 both activate Wnt signalling, but FAM83F acts upstream of the β -catenin destruction complex, while FAM83G/PAWS1 acts downstream (6). The specific CK1 α substrates within the canonical Wnt signalling pathway which mediate the effects of both FAM83F and FAM83G/PAWS1 are unknown.

Phosphorylation of β -catenin by CK1 α at Ser45 is the most established regulatory role of CK1 α within the Wnt pathway and is critical for priming subsequent GSK-3 phosphorylation, ubiquitination and degradation of β -catenin and thus inhibition of Wnt signalling (29). P120-catenin is one of the few reported Wnt-dependent CK1 α substrates located at the plasma

membrane. The sequential phosphorylation of P120-catenin, at the adherens junctions by CK1 ϵ and CK1 α is required for the internalisation of the Wnt signalosome (17). The contradictory nature of the CK1 isoforms in Wnt signalling can be demonstrated by the CK1 δ/ϵ isoforms which have been reported to phosphorylate multiple proteins within the Wnt signalling pathway including Dishevelled (30) and a co-transcriptional regulator, lymphoid enhanced binding factor 1 (Lef-1) (31). Interestingly, phosphorylation of Dishevelled at the membrane following Wnt stimulation promotes signalling whilst phosphorylation of Lef-1 in the nucleus is inhibitory, thus the same kinase can have opposing actions depending on subcellular localisation. It will be interesting to determine whether and how different FAM83 proteins coordinate the phosphorylation of these and other CK1 substrates to finetune Wnt signalling.

FAM83F has been implicated in oncogenesis in several cancers (12, 14, 32), and increased abundance of FAM83F protein is also associated with a more aggressive phenotype and poor prognosis in oesophageal carcinoma (33). However, a mechanistic explanation for these oncogenic effects has not been forthcoming. We show here that overexpression of FAM83F protein in cells increases both basal and ligand-dependent canonical Wnt signalling which may explain the reported increase in cell proliferation. FAM83F has also been implicated in the stabilisation of p53 protein, a crucial tumour suppressor, by decreasing p53 ubiquitination and degradation (34). This stabilisation is also apparent with mutant p53 protein, thus FAM83F may have a tumour suppressor or an oncogenic role depending on the p53 mutational status of the cell (34). Interestingly, CK1 α has also been reported to influence p53 stabilisation through binding to the E3 ligases MDM2 (35) and MDMX (36) which inhibit p53 activity through ubiquitination and direct binding respectively. Therefore, these reported p53 effects may potentially be another function of the FAM83F-CK1 α complex. The potential regulation of both canonical Wnt signalling and p53 activity indicates that further investigation of the FAM83F-CK1 α complex is required and given the common dysregulation of both Wnt and p53 signalling during oncogenesis, the FAM83F-CK1 α complex may be an attractive therapeutic target in cancer progression.

MATERIALS & METHODS

Plasmids

All constructs are available for request from the MRC-PPU reagents website (<http://mrcpppureagents.dundee.ac.uk>) with the unique identifier (DU) numbers providing direct links to cloning strategy and sequence information. Sequences were verified by the DNA sequencing service, University of Dundee (<http://www.dnaseq.co.uk>). Constructs generated include; pcDNA5-FRT/TO GFP only (DU41455), pcDNA5-FRT/TO GFP FAM83A (DU44235), pcDNA5-FRT/TO GFP FAM83B (DU44236), pcDNA5-FRT/TO GFP FAM83C (DU42473), pcDNA5-FRT/TO GFP FAM83D (DU42446), pcDNA5-FRT/TO GFP FAM83E (DU44237), pcDNA5-FRT/TO GFP FAM83F (DU44238), pcDNA5-FRT/TO GFP FAM83G (DU33272), pcDNA5-FRT/TO GFP FAM83H (DU44239), pcDNA5-FRT/TO GFP FAM83F^{C497A} (DU28157), pcDNA5-FRT/TO GFP FAM83F^{D250A} (DU28268), pcDNA5-FRT/TO GFP FAM83F^{F284A/F288A} (DU28260), pBABED.puro U6 FAM83F tv1 Nter KI sense (DU54050), pX335 FAM83F Nter KI Antisense (DU54056), pMS-RQ FAM83F Nter GFP donor (DU54325), pBABED.puro U6 FAM83F ex2 KO sense (DU54848), pX335 FAM83F ex2 KO Antisense (DU54850), pBABED.puro U6 FAM83F Cter KI Sense A (DU60633), pX335 FAM83F Cter KI Antisense A (DU60635) and pMA FAM83F Cter C497A IRES GFP donor (DU60711).

To amplify plasmids, 10 µl of *E. coli* DH5α competent cells (Invitrogen) were transformed using 1 µl of plasmid DNA. The bacteria were incubated on ice for 10 min, heat-shocked at 42°C for 45 s and then incubated in ice for a further 2 min. Transformed bacteria were spread on ampicillin (100 µg/ml) containing LB-agar medium plates and incubated at 37°C for 16 h. A 5 ml culture of ampicillin (100 µg/ml) containing LB medium was inoculated with a single bacteria colony and incubated at 37°C for 16 h with constant shaking. Following bacterial growth, the bacteria were pelleted and plasmid DNA was purified using QIAprep Spin Miniprep kit (27104, Quigen) following the manufacturer's instructions. A Nanodrop 1000 spectrophotometer (Thermo Scientific) was used to determine isolated DNA yield.

Antibodies

Antibodies recognising GFP (S268B), CK1α (SA527), CK1δ (SA609), CK1ε (SA610) and FAM83F (SA103) are available for request from the MRC-PPU reagents website (<http://mrcpppureagents.dundee.ac.uk>). Antibodies for β-actin (#4967), GAPDH (14C10) (#2118), p-LRP6 (S1490) (#2568), LRP6 (C47E12) (#3395), β-catenin (D10A8) (#8480), phospho-β-catenin (S45) (#9564), phospho-β-catenin (S33/S37/T41) (#9561), Na/K ATPase (D4Y7E) (#23565) and Lamin A/C (#2032) were purchased from Cell signalling technology.

Additional antibodies used were FAM83G (Abcam, ab121750), Alpha-tubulin (Thermo-Fisher Scientific, MA1-80189), Active- β -catenin (anti-ABC) clone 8E7 (END Millipore, 05-665), mouse anti-GFP clone 7.1 and 13.1 (Roche), mouse-monoclonal anti-HA (Sigma, H9658) and U2AF1 (Thermo-Fisher Scientific, PA5-28510). Secondary antibodies used were StarBright Blue 700 Goat anti-Rabbit IgG (Bio-Rad, 12004161), StarBright Blue 700 Goat anti-Mouse IgG (Bio-Rad, 12004158), IRDye 800CW Donkey anti-Goat IgG (LI-COR, 926-32214), IRDye 800CW Goat anti-Rat IgG (LI-COR, 926-32219), IRDye 800CW Goat anti-Mouse (LI-COR 926-32210) and IRDye 680LT Goat anti-Rabbit (LI-COR, 926-68021)

Constructs and mRNA synthesis for *Xenopus* assays

Coding sequences for the opening reading frames (ORFs) of *fam83fa* and *fam83fb* were obtained from the Ensembl genome browser (Ensembl release 87 - December 2016 © [EMBL-EBI](#), GRCz9). Primers were designed to amplify the ORFs to clone into pENTR/D-TOPO entry vectors (Invitrogen) according to the manufacturer's instructions. For *fam83fa*, the template was amplified from a previously prepared zebrafish cDNA library; for *fam83fb* an I.M.A.G.E. clone (7048616) (Dharmacon) was used. Inserts were then subcloned into pCS2+ N' HA tagged vectors that had been converted into Gateway® (Invitrogen) destination vectors, according to the manufacturer's instructions. Mutant constructs (*fam83fa*^{F275A}, *fam83fa*^{F279A} and *fam83fa*^{F275/279A}) were generated by site-directed mutagenesis using the Q5® Site-Directed Mutagenesis Kit (NEB) according to the manufacturer's instructions. C' terminal truncation constructs (*fam83fa*^{1-500aa}, *fam83fa*^{1-400aa}, *fam83fa*^{1-356aa} and *fam83fa*^{1-300aa (DUF)}) were generated by pENTR/D-TOPO cloning as previous, using reverse primers designed accordingly. The human FAM83F WT and CAAX box mutant constructs were made by Kevin Dingwell. All constructs were Sanger sequenced by the Genomics Equipment Park Science Technology Platform at the Crick. For mRNA synthesis, PCR templates for *in vitro* transcription were generated from the pCS2+ N' HA tagged destination vectors. Templates were then used in an SP6 mMessage mMachine (Invitrogen) transcription reaction to generate capped mRNAs.

***Xenopus laevis* maintenance, microinjection and western blotting**

All *Xenopus laevis* work, including housing and husbandry, was undertaken in accordance with The Crick Use of Animals in Research Policy, the Animals (Scientific Procedures) Act 1986 (ASPAs) implemented by the Home Office in the UK and the Animal Welfare Act 2006. Consideration was given to the '3Rs' in experimental design. *Xenopus laevis* embryos were obtained by *in vitro* fertilisation and staged according to Nieuwkoop and Faber (1994) (37). Embryos were maintained in Normal Amphibian Medium (NAM) (38) until the four-cell stage was reached, at which point they were injected with 500 pg of the indicated capped mRNA

into a single ventral blastomere. Embryos were allowed to develop until ~stage 35 at which point they were fixed in 4% paraformaldehyde. Embryos were then counted and scored for secondary axial phenotype classes as shown.

For Western blotting, embryos were obtained as above and injected into the animal hemisphere at the one-cell stage with 500 pg of the indicated capped mRNA. Embryos were allowed to develop to stage 10 before being lysed in 10 μ l/embryo ice-cold lysis buffer (1% IGEPAL, 150 mM NaCl, 10 mM HEPES pH 7.4, 2 mM EDTA, protease inhibitor cocktail (Pierce, A32965)). Lipids and yolk were removed from the lysate by FREON extraction (equal volume), the aqueous phase was collected following centrifugation for 15 minutes at 4°C. Protein extracts were then denatured in SDS buffer before being separated by SDS-PAGE (or snap-frozen on dry ice and stored at -80°C for later). Proteins were then transferred onto a LF-PVDF (LI-COR) membrane and blocked in Odyssey blocking buffer in TBS (LI-COR) for 1 hr at RT. Blots were then incubated overnight at 4°C in primary antibodies diluted in Odyssey blocking buffer. Following TBST washes, blots were then incubated in secondary antibodies diluted in TBST with 0.02% SDS. Blots were then imaged using the LI-COR Odyssey imaging system in 700 and 800 nm channels and processed for brightness and contrast in Adobe Photoshop CC (2019).

Cell culture

U2OS (HTB-96, ATCC), HCT116 (CCL-247, ATCC), DLD-1 (CCL-221, ATCC), mouse fibroblast L-cells that stably overexpress Wnt3A (CRL-2647, ATCC), mouse fibroblast L cells (CRL-2648, ATCC), Flp-In T-Rex U2OS (which were created using Flp-In T-Rex Core kit (K650001, Thermo Fisher Scientific) and have been previously reported (1)), Flp-In T-Rex HEK293 (R78007, Thermo Fisher Scientific) and HaCaT (obtained from Joan Massagué's lab at Memorial Sloan Kettering Cancer Centre, not commercially available but can be provided on request) (39) cells were maintained in Dulbecco's Modified Eagle's Medium (DMEM; Gibco) containing 10 % FCS (Hyclone), 100 U/ml penicillin (Lonza), 100 mg/ml streptomycin (Lonza) and 2 mM L-glutamine (Lonza). Cell lines were routinely tested for mycoplasma contamination and only mycoplasma free cell lines were used for experimentation. The additional cell lines reported in Supplementary Figure 4 were kindly donated by various research groups within the MRC-PPU facility (University of Dundee) in the form of cell pellets and were immediately lysed to determine protein abundance.

Generation of stable Flp-In T-rex cell lines

The Flp-In T-Rex U2OS were transfected with the N-terminal GFP-tagged FAM83A, FAM83B, FAM83C, FAM83D, FAM83E, FAM83F, FAM83G, FAM83H, FAM83F^{C497A}, FAM83F^{D250A}, FAM83F^{F284/288A} or GFP only packaged in a pcDNA5-FRT/TO vector, along with Flp recombinase pOG44 (Invitrogen) in a ratio of 1 µg : 9 µg. The Flp-In T-Rex HEK293 cells were transfected with the N-terminal GFP-tagged FAM83F packaged in a pcDNA5-FRT/TO vector along with Flp recombinase pOG44 (Invitrogen) in a ratio of 1 µg : 9 µg. Plasmids were diluted in 1 ml of OptiMem (Gibco) and 20 µl polyethylenimine (PEI; 1 mg/ml) (Polysciences) was added. The transfection mixture was vortexed and incubated for 20 min at room temperature before adding dropwise to a 10-cm diameter dish of cells in complete culture medium. Selection of cells was performed 24 h post transfection with the addition of 50 µg/ml hygromycin and 15 µg/ml blasticidin to complete culture medium. Resistant cells were grown to confluency and tested for expression by Western blotting. Expression was induced by incubating cells in 20 ng/ml doxycycline for 24 h.

Generation of FAM83F^{-/-}, GFP/GFP FAM83F and FAM83F^{WT/C497A} cell lines using

CRISPR/Cas9. FAM83F knock-out HCT116 (clone.1), DLD-1, U2OS and HaCaT cell lines were generated by targeting the *FAM83F* locus with a dual guide RNA approach using the sense guide RNA (pBabeD-puro vector, DU54848); GCGTCCAGGATGATGTACACT and antisense guide RNA (pX335-Cas9-D10A vector, DU54850); GGCAGGAGTGAAGTATTTCC. N-terminal GFP knock-in to the *FAM83F* locus in HCT116 and DLD-1 cells were generated by targeting the *FAM83F* locus with a dual guide RNA approach using the sense guide RNA (pBabeD-puro vector, DU54050); GTTCAGCTGGGACTCGGCCA, antisense guide RNA (pX335-Cas9-D10A vector, DU54056); GCGAGGCGCACGTGAACGAGA and the GFP-FAM83F donor (pMK-RQ vector, DU54325). FAM83F^{-/-} HCT116 (clone.2) was generated by the targeting of the N-terminus of FAM83F with the intention of knocking in a GFP tag, but this clone did not incorporate the GFP donor plasmid and after inefficient repair of the cut DNA the clone was null for FAM83F protein expression. HCT116 FAM83F^{C497A} knockin cell lines were generated by targeting the C-terminal of *FAM83F* with a dual guide RNA approach using the sense guide RNA (pBabeD-puro vector, DU60633), antisense guide RNA (pX335-Cas9-D10A vector, 60635) and FAM83F C-terminal donor containing C497A mutation (pMA vector, DU60711). The donor plasmid contained an internal ribosome entry site (IRES) after the stop codon following the FAM83F C497A sequence and was followed by a GFP sequence to aid selection of positive clones.

For transfection, plasmids (1 µg of guide RNAs +/- 3 µg donor) were diluted in 1 ml OptiMem (Gibco) and 20 µl PEI (1 mg/ml). The transfection mixture was vortexed for 15 s and incubated for 20 min at room temperature. This mixture was then added dropwise to a 10-cm diameter dish containing approximately 70% confluent cells in complete culture medium. Transfected cells were selected 24 h post transfection with the addition of 2 µg/ml puromycin to complete culture medium for 48 h. Single cells were isolated by fluorescence-activated cell sorting (FACS) with single GFP-positive cells (for knock-in strategies) or all single cells (for knock-out strategies) plated in individual wells of a 96-well plate, pre-coated with 1% (w/v) gelatin (Sigma). Viable clones were expanded and screened by Western blotting for efficient knock-in or knock-out.

Knock-in and knock-out clones were verified by DNA sequencing. DNA was isolated from cell pellets using the DNeasy Blood & Tissue kit (69505, Qiagen). Primers were generated to amplify the surrounding region of the guide RNA target sites with the following primer pairs: FAM83F KO exon 2 (Forward: TCATTGCTGTGGTCATGGAC, Reverse: AATCCGGAAGTCAGTGAGCT), FAM83F N-terminal GFP KI (Forward: TGTACAAGGCCGAGAGTCAGCTGAACTG, Reverse: CAGTTCAGCTGACTCTCGGCCTTG TACA). The region was amplified by polymerase chain reaction (PCR) with KOD Hot Start Polymerase (Merck) according to manufacturer's instructions. The PCR products of positive clones were then cloned into competent cells using the StrataClone PCR Cloning Kit (Agilent) according to the manufacturer's protocol. Isolation of DNA and sequencing was performed by the MRC-PPU DNA sequencing and services (<http://mrcppureagents.dundee.ac.uk>).

Generation of L- and Wnt3A- conditioned media

Conditioned media were generated from mouse fibroblast L-cells and mouse fibroblast L-cells that stably overexpress Wnt3A. L-cells and L-Wnt3A cells were grown in DMEM in 15-cm diameter dishes for 3 days before medium was filtered (45 µm) and stored as L-conditioned media (L-CM) and Wnt3A-conditioned media (Wnt3A-CM). Conditioned medium was diluted 50:50 in DMEM containing 10% FCS before use.

Compound treatments

CHIR99021 (Tocris), a highly selective Glycogen Synthase Kinase 3 (GSK-3) inhibitor, was added to cells at a concentration of 5 µM for 6 h prior to lysis.

Protein extraction from cells

Cells were washed in PBS twice, scraped in PBS and pelleted. For whole cell protein extractions, cell pellets were resuspended in total lysis buffer (20 mM Tris-HCl (pH 7.5), 150 mM NaCl, 1 mM Na₂EDTA, 1 mM EGTA, 1% (v/v) Triton X-100, 2.5 mM sodium pyrophosphate, 1 mM beta-glycerophosphate, 1 mM Na₃VO₄, 1x complete EDTA-free protease inhibitor cocktail (Roche)). Lysates were incubated on ice for 30 min and vortexed regularly then clarified at 13000 rpm for 20 min. For cellular fractionation, cell pellets were washed in PBS twice, scraped in PBS, pelleted and then separated into cytoplasmic, nuclear and membrane lysates using a subcellular protein fractionation kit (Thermo Fisher Scientific) following the manufacturer's protocol. Briefly, cell pellets were resuspended in sequential buffers and clarified to isolate specific cellular compartments (cytoplasmic, nuclear, membrane and cytoskeletal).

Protein extraction from mouse tissue

Mouse tissue samples were obtained from a single male C57BL/6j mouse, which was obtained from the MRC-PPU after it was designated as surplus to current breeding requirements and culled by schedule one methods. Tissue samples were dissected, washed in PBS and snap frozen in liquid nitrogen. Frozen tissue samples were ground using a mortar and pestle until the sample was a fine powder which was then resuspended in PBS and pelleted. This pellet was resuspended in total lysis buffer (20 mM Tris-HCl (pH 7.5), 150 mM NaCl, 1 mM Na₂EDTA, 1 mM EGTA, 1% (v/v) Triton X-100, 2.5 mM sodium pyrophosphate, 1 mM beta-glycerophosphate, 1 mM Na₃VO₄, 1x complete EDTA-free protease inhibitor cocktail (Roche)). Lysates were incubated on ice for 45 min and vortexed regularly before clarifying at 13000 rpm for 20 min.

For the isolation of single crypts from the mouse small intestine, a section of proximal small intestine was washed in PBS then cut into small fragments. Further washing of the fragments in PBS was completed until minimal contamination remained. The intestinal fragments were incubated in 3 mM EDTA for 30 min at 4°C on a rotating wheel to dissociate the crypts. The EDTA was removed and the fragments gently washed in PBS before washing the fragments more aggressively in PBS to dislodge the crypts. Crypts were collected as a component of the supernatant. Crypts were pelleted at 800 rpm for 5 min. The pellet was resuspended in total cell lysis buffer (20 mM Tris-HCl (pH 7.5), 150 mM NaCl, 1 mM Na₂EDTA, 1 mM EGTA, 1% (v/v) Triton X-100, 2.5 mM sodium pyrophosphate, 1 mM beta-glycerophosphate, 1 mM Na₃VO₄, 1x complete EDTA-free protease inhibitor cocktail (Roche)). Lysates were incubated on ice for 30 min with regular vortexing and clarified at 13000 rpm for 20 min.

SDS-PAGE and Western blotting

The protein concentration of lysates was measured using the Pierce Coomassie Bradford protein assay kit (Thermo Fisher Scientific). Final protein concentrations were adjusted to 1-3 µg/µl in lysis buffer and NuPAGE 4x LDS sample buffer (NP0007, Thermo Fisher Scientific) was added to a final concentration of 1x and lysates were denatured at 95°C for 5 min. Lysates (20-40 µg protein) were separated by sodium dodecyl sulphate-polyacrylamide (SDS-PAGE) gels and transferred to 0.2 µm pore size nitrocellulose membrane (1620112, BioRad). Following washing in TBS-T (50 mM Tris-HCL (pH 7.5), 150 mM NaCl, 0.1% (v/v) Tween 20) membranes were incubated in 5% (w/v) milk in PBS for 60 min. Membranes were washed in TBS-T, then incubated in primary antibody (diluted 1:500-1:1000 in 5% (v/v) milk in TBS-T) for 16 h at 4°C. Membranes were washed in TBS-T (3x10 min), incubated in secondary antibody (diluted 1:5000 in 5% (v/v) milk in TBS-T) for 1 h at room temperature and then washed in TBS-T (3x10 min). Detection of fluorescent secondary antibody was performed using the Chemidoc system (BioRad) and Image lab software (BioRad). Densitometry of protein blots was completed, using Image J software (<https://imagej.net>), by measuring the density of protein of interest bands and normalising to that of the corresponding loading control bands. Statistical analysis and preparation of graphs was completed using Microsoft Excel software (www.microsoft.com) and Prism 8 (www.graphpad.com) respectively.

Immunoprecipitation

Lysates were prepared and protein concentrations quantified as described previously. For GFP immunoprecipitations (IPs), 10 µl of pre-equilibrated GFP-Trap Agrose beads (Chromotek) were added to each lysate sample (1 mg protein) and incubated on a rotating wheel for 16 h at 4°C. For antibody-IPs, either anti-CK1α (1 µg) or anti-FAM83F (1 µg) antibody was added to each lysate sample (1 mg protein), incubated on a rotating wheel for 16 h at 4°C and then 20 µl of pre-equilibrated Protein G Sepharose beads (50% beads:lysis buffer slurry) (DSTT) were added to each lysate sample and incubated on a rotating wheel for 1 h at 4°C. Following incubation of the lysate with beads, the beads were pelleted and the supernatant was removed and stored as flow-through. Beads were washed in lysis buffer three times before eluting proteins by the addition of 20-40 µl of NuPAGE 1x LDS sample buffer to the beads and denaturing proteins by incubating at 95°C for 10 min. The input (IN) and eluted samples (IP) were separated by SDS-PAGE and subjected to Western blotting with antibodies as previously outlined.

Immunofluorescence

Cells were plated in 12-well plates containing sterile glass coverslips. Cells were incubated for 24 h before removing medium and incubating cells in 4% paraformaldehyde for 15 min to fix. Following fixation, cells were permeabilized in 0.2% Triton X-100 for 10 min, incubated in blocking buffer (5% (w/v) bovine serum albumin in PBS) for 60 min and then washed in TBS-T before incubating in primary antibody. The following primary antibodies were diluted in 0.5% (w/v) bovine serum albumin in TBS-T and incubated for 16 h at 4°C: mouse anti-GFP (1:1000) (Roche), sheep anti-CK1 α (1:100) (DSTT), rabbit anti- β -catenin (1:250) (CST) or sheep anti-FAM83F (1:250) (DSTT). Coverslips were washed in PBS/0.1% Tween-20 (3x10 min) then incubated in Alexa Fluor 488 phalloidin, Alexa Fluor donkey anti-mouse 488 secondary, Alexa Fluor donkey anti-sheep 594 secondary, Alexa Fluor donkey anti-sheep 488 secondary or Alexa Fluor donkey anti-rabbit 594 secondary (Thermo Fisher Scientific) diluted (1:500) in 0.5% (w/v) bovine serum albumin in PBS/0.1% Tween-20 for 60 min at room temperature. Coverslips were washed in PBS/0.1% Tween-20 (3x10 min), incubated in 1 μ g/ml DAPI diluted in PBS/0.1% Tween-20 for 5 min at room temperature before further washing in PBS/0.1% Tween-20 (3x5 min). Coverslips were mounted and sealed on glass slides using Vectashield mounting medium (Vector Laboratories) and CoverGrip coverslip sealant (Biotium) respectively. Fluorescence images were captured using a Deltavision microscope with a 60x objective. Images were prepared for publication using the Omero software (www.openmicroscopy.org).

Dual luciferase reporter assays

Cells were plated in 6-well plates and grown to approximately 70% confluence in complete culture medium. Cells were transfected with either 500 ng of Super TOPFlash (Addgene) or Super FOPFlash (Addgene) luciferase plasmids plus 10 ng of Renilla (Addgene) luciferase plasmids. Plasmids were diluted in 1 ml OptiMem (Gibco) and 20 μ l of PEI (1 mg/ml) was added. The transfection mixture was vortexed then incubated for 20 min at room temperature before adding dropwise to a 6-well plate of cells in complete culture medium. Following transfection (24 h), cells were treated with either L-conditioned medium or L-Wnt3A-conditioned medium for 6 h. Cells were washed in PBS twice and lysed in passive lysis buffer (Promega, #E194A) for 15 min on rocker. After lysis, 20 μ l of lysate was transferred to triplicate wells in a white bottom 96-well plate and then 20 μ l of 2x luciferase assay buffer (50 mM Tris/Phosphate, 16 mM MgCl₂, 2 mM DTT, 1 mM ATP, 30% (v/v) Glycerol, 1% (w/v) BSA, 0.25 mM D-luciferin, 8 μ M Sodium Pyrophosphate) was added to each well, incubated for 2 min, and absorbance at 560 nm measured. Immediately after reading absorbance, 20 μ l of 3x Renilla buffer (45 mM Na₂EDTA, 30 mM Sodium Pyrophosphate, 1.425 M NaCl, 0.06 mM PTC124, 0.01 mM h-CTZ) was added to each well

and incubated for 5 min before absorbance at 560 nm was again measured. The luciferase absorbance counts were normalised to Renilla absorbance counts, which represent a measure of transfection efficiency.

Quantitative real time polymerase chain reaction (qRT-PCR)

Cells were plated in 6-well plates and grown to approximately 70% confluence in complete culture medium, then conditioned-medium or treatment added as indicated. RNA extractions were completed using RNeasy mini kit (74104, Qiagen) following the manufacturer's instructions and RNA was quantified using a NanoDrop 3300 Fluorospectrometer (Thermo Fisher Scientific). Synthesis of complementary DNA (cDNA) was completed using 1 µg of RNA and the iScript cDNA synthesis kit (BioRad). Each qRT-PCR was performed as triplicate reactions with the following reaction mixture: 2 µM forward primer, 2 µM reverse primer, 50% (v/v) iQ SYBR green supermix (BioRad) and 2 µl cDNA (diluted 1:5) in a 10 µl final volume. Reactions were completed on a CFX384 real-time system qRT-PCR machine (BioRad). Primers were designed using Benchling (www.benchling.com) and purchased from Invitrogen. *Axin2* forward: TACACTCCTTATTGGGCGATCA, *Axin2* reverse: TTGGCTACTCGTAAAGTTTTGGT, *GAPDH* forward: TGCACCACCAACTGCTTAGC, *GAPDH* reverse: GGCATGGACTGTGGTCATGAG. The comparative Ct method ($\Delta\Delta C_t$ Method) was used to analyse the datasets with *Axin2* the Wnt target gene and *GAPDH* the endogenous control gene. Statistical analysis and preparation of graphs was completed using Microsoft Excel software (www.microsoft.com) and Prism 8 (www.graphpad.com) respectively.

Acknowledgements

We thank E. Allen, L. Fin, J. Stark and A. Muir for help and assistance with tissue culture, the staff at the DNA sequencing services (School of Life Sciences, University of Dundee), the cloning, antibody and protein production teams within the MRC-PPU reagents and services (University of Dundee), coordinated by J. Hastie. We thank the staff at the Dundee Imaging Facility (School of Life Sciences, University of Dundee) for their invaluable help and advice throughout this project. We thank the Crick Aquatics Team (BRF STP) for *Xenopus* care and husbandry and the Crick Genomics Equipment Park for Sanger sequencing services. We thank all members of the Sapkota and Smith labs for their highly appreciated experimental advice and/or discussions.

Funding

Karen Dunbar is supported by an MRC Career Development Fellowship. GPS is supported by the U.K. Medical Research Council (grant number MC_UU_00018/6 and MC_UU_12016/3) and the pharmaceutical companies supporting the DSTT (Boehringer-Ingelheim, GlaxoSmithKline, Merck-Serono). RAJ, Kevin Dingwell and JCS are supported by the Francis Crick Institute, which receives its core funding from Cancer Research UK [FC001-157], the UK MRC [FC001-157], and the Wellcome Trust [FC001-157].

Author contributions

Karen Dunbar performed experiments, collected and analysed data, and contributed to the writing of the manuscript. RAJ performed *Xenopus* experiments, collected and analysed data, and contributed to the writing of the manuscript. Kevin Dingwell performed experiments, collected and analysed data. TJM designed strategies and developed methods for the CRISPR/Cas9 gene editing, in addition to generating constructs used in this study. JCS provided project supervision, analysed data and contributed to the writing of the manuscript. GPS conceived the project, provided project supervision, analysed data and contributed to the writing of the manuscript.

REFERENCES

1. Fulcher LJ, Bozatz P, Tachie-Menson T, Wu KZL, Cummins TD, Bufton JC, et al. The DUF1669 domain of FAM83 family proteins anchor casein kinase 1 isoforms. *Sci Signal*. 2018;11(531).
2. Schitteck B, Sinnberg T. Biological functions of casein kinase 1 isoforms and putative roles in tumorigenesis. *Mol Cancer*. 2014;13:231.
3. Cruciat CM. Casein kinase 1 and Wnt/ β -catenin signaling. *Curr Opin Cell Biol*. 2014;31:46-55.
4. Jiang S, Zhang M, Sun J, Yang X. Casein kinase 1 α : biological mechanisms and theranostic potential. *Cell Commun Signal*. 2018;16(1):23.
5. Philpott JM, Narasimamurthy R, Ricci CG, Freeberg AM, Hunt SR, Yee LE, et al. Casein kinase 1 dynamics underlie substrate selectivity and the PER2 circadian phosphoswitch. *Elife*. 2020;9.
6. Bozatz P, Dingwell KS, Wu KZ, Cooper F, Cummins TD, Hutchinson LD, et al. PAWS1 controls Wnt signalling through association with casein kinase 1 α . *EMBO Rep*. 2018;19(4).
7. Wu KZL, Jones RA, Tachie-Menson T, Macartney TJ, Wood NT, Varghese J, et al. Pathogenic FAM83G palmoplantar keratoderma mutations inhibit the PAWS1:CK1 α association and attenuate Wnt signalling. *Wellcome Open Res*. 2019;4:133.
8. Fulcher LJ, He Z, Mei L, Macartney TJ, Wood NT, Prescott AR, et al. FAM83D directs protein kinase CK1 α to the mitotic spindle for proper spindle positioning. *EMBO Rep*. 2019;20(9):e47495.
9. Kim JW, Lee SK, Lee ZH, Park JC, Lee KE, Lee MH, et al. FAM83H mutations in families with autosomal-dominant hypocalcified amelogenesis imperfecta. *Am J Hum Genet*. 2008;82(2):489-94.
10. Tachie-Menson T, Gázquez-Gutiérrez A, Fulcher LJ, Macartney TJ, Wood NT, Varghese J, et al. Characterisation of the biochemical and cellular roles of native and pathogenic amelogenesis imperfecta mutants of FAM83H. *Cell Signal*. 2020;72:109632.
11. Xu L, Yu QW, Fang SQ, Zheng YK, Qi JC. MiR-650 inhibits the progression of glioma by targeting FAM83F. *Eur Rev Med Pharmacol Sci*. 2018;22(23):8391-8.
12. Fan G, Xu P, Tu P. MiR-1827 functions as a tumor suppressor in lung adenocarcinoma by targeting MYC and FAM83F. *J Cell Biochem*. 2019.
13. Mao Y, Liu J, Zhang D, Li B. miR-143 inhibits tumor progression by targeting FAM83F in esophageal squamous cell carcinoma. *Tumour Biol*. 2016;37(7):9009-22.
14. Fuziwara CS, Saito KC, Leoni SG, Waitzberg Â, Kimura ET. The Highly Expressed FAM83F Protein in Papillary Thyroid Cancer Exerts a Pro-Oncogenic Role in Thyroid Follicular Cells. *Front Endocrinol (Lausanne)*. 2019;10:134.
15. Komiya Y, Habas R. Wnt signal transduction pathways. *Organogenesis*. 2008;4(2):68-75.
16. Verheyen EM, Gottardi CJ. Regulation of Wnt/ β -catenin signaling by protein kinases. *Dev Dyn*. 2010;239(1):34-44.
17. Vinyoles M, Del Valle-Pérez B, Curto J, Viñas-Castells R, Alba-Castellón L, García de Herreros A, et al. Multivesicular GSK3 sequestration upon Wnt signaling is controlled by p120-catenin/cadherin interaction with LRP5/6. *Mol Cell*. 2014;53(3):444-57.

18. Jho EH, Zhang T, Domon C, Joo CK, Freund JN, Costantini F. Wnt/beta-catenin/Tcf signaling induces the transcription of Axin2, a negative regulator of the signaling pathway. *Mol Cell Biol*. 2002;22(4):1172-83.
19. Network CGA. Comprehensive molecular characterization of human colon and rectal cancer. *Nature*. 2012;487(7407):330-7.
20. Kühl M, Pandur P. Dorsal axis duplication as a functional readout for Wnt activity. *Methods Mol Biol*. 2008;469:467-76.
21. Gao J, Liao J, Yang GY. CAAX-box protein, prenylation process and carcinogenesis. *Am J Transl Res*. 2009;1(3):312-25.
22. Sebti SM. Protein farnesylation: implications for normal physiology, malignant transformation, and cancer therapy. *Cancer Cell*. 2005;7(4):297-300.
23. Xie Y, Zheng Y, Li H, Luo X, He Z, Cao S, et al. GPS-Lipid: a robust tool for the prediction of multiple lipid modification sites. *Sci Rep*. 2016;6:28249.
24. Ishitani T, Ninomiya-Tsuji J, Nagai S, Nishita M, Meneghini M, Barker N, et al. The TAK1-NLK-MAPK-related pathway antagonizes signalling between beta-catenin and transcription factor TCF. *Nature*. 1999;399(6738):798-802.
25. Korinek V, Barker N, Morin PJ, van Wichen D, de Weger R, Kinzler KW, et al. Constitutive transcriptional activation by a beta-catenin-Tcf complex in APC-/- colon carcinoma. *Science*. 1997;275(5307):1784-7.
26. Fodde R. The APC gene in colorectal cancer. *Eur J Cancer*. 2002;38(7):867-71.
27. Yang J, Zhang W, Evans PM, Chen X, He X, Liu C. Adenomatous polyposis coli (APC) differentially regulates beta-catenin phosphorylation and ubiquitination in colon cancer cells. *J Biol Chem*. 2006;281(26):17751-7.
28. Wang Z, Vogelstein B, Kinzler KW. Phosphorylation of beta-catenin at S33, S37, or T41 can occur in the absence of phosphorylation at T45 in colon cancer cells. *Cancer Res*. 2003;63(17):5234-5.
29. Amit S, Hatzubai A, Birman Y, Andersen JS, Ben-Shushan E, Mann M, et al. Axin-mediated CKI phosphorylation of beta-catenin at Ser 45: a molecular switch for the Wnt pathway. *Genes Dev*. 2002;16(9):1066-76.
30. Bernatik O, Ganji RS, Dijksterhuis JP, Konik P, Cervenka I, Polonio T, et al. Sequential activation and inactivation of Dishevelled in the Wnt/beta-catenin pathway by casein kinases. *J Biol Chem*. 2011;286(12):10396-410.
31. Hämmerlein A, Weiske J, Huber O. A second protein kinase CK1-mediated step negatively regulates Wnt signalling by disrupting the lymphocyte enhancer factor-1/beta-catenin complex. *Cell Mol Life Sci*. 2005;62(5):606-18.
32. Gu GM, Zhan YY, Abuduwaili K, Wang XL, Li XQ, Zhu HG, et al. MiR-940 inhibits the progression of NSCLC by targeting FAM83F. *Eur Rev Med Pharmacol Sci*. 2018;22(18):5964-71.
33. Yang H, Wei YN, Zhou J, Hao TT, Liu XL. MiR-455-3p acts as a prognostic marker and inhibits the proliferation and invasion of esophageal squamous cell carcinoma by targeting FAM83F. *Eur Rev Med Pharmacol Sci*. 2017;21(14):3200-6.
34. Salama M, Benitez-Riquelme D, Elabd S, Munoz L, Zhang P, Glanemann M, et al. Fam83F induces p53 stabilisation and promotes its activity. *Cell Death Differ*. 2019;26(10):2125-38.
35. Huart AS, MacLaine NJ, Meek DW, Hupp TR. CK1alpha plays a central role in mediating MDM2 control of p53 and E2F-1 protein stability. *J Biol Chem*. 2009;284(47):32384-94.

36. Wu S, Chen L, Becker A, Schonbrunn E, Chen J. Casein kinase 1 α regulates an MDMX intramolecular interaction to stimulate p53 binding. *Mol Cell Biol.* 2012;32(23):4821-32.
37. J NPDaF. Normal table of *Xenopus laevis* (Daudin): a systematical and chronological survey of the development from the fertilized egg till the end of metamorphosis. New York: Garland Publishing, Inc.; 1994.
38. Slack JM. Regional biosynthetic markers in the early amphibian embryo. *J Embryol Exp Morphol.* 1984;80:289-319.
39. Sapkota G, Alarcón C, Spagnoli FM, Brivanlou AH, Massagué J. Balancing BMP signaling through integrated inputs into the Smad1 linker. *Mol Cell.* 2007;25(3):441-54.

FIGURE LEGENDS

Figure 1: Fam83f induces axis duplication in *Xenopus* embryos through an interaction with CK1 α .

(A) Brightfield microscopy images of *Xenopus* embryo axis duplication phenotypes; wild-type, dorsalisated, partial secondary axis and complete secondary axis. **(B)** Percentage of *Xenopus* embryos showing the phenotypes in (A) following injection with HA tagged zebrafish *fam83fa* or *fam83fb* mRNA. Data represents one independent experiment with numbers of *Xenopus* embryos denoted above the graph. **** $p < 0.0001$, Chi-squared test. **(C)** Protein extracts from *Xenopus* embryos following injection with either HA-*fam83fa* or HA-*fam83fb* mRNA, were resolved by SDS-PAGE and subjected to Western blotting with indicated antibodies. **(D)** Percentage of *Xenopus* embryos showing phenotypes depicted in (A) following injection with HA tagged zebrafish *fam83fa*, *fam83fa*^{F275A}, *fam83fa*^{F279A} or *fam83fa*^{F275/279A} mRNA. Data represents three independent experiments with total numbers of *Xenopus* embryos denoted above the graph. Bar graph representing mean + standard deviation. **** $p < 0.0001$, two-way ANOVA with Tukey's post-hoc test to compare the percentage of embryos displaying a wild-type phenotype. **(E)** Protein extracts from *Xenopus* embryos following injection with HA tagged zebrafish *fam83fa*, *fam83fa*^{F275A}, *fam83fa*^{F279A} or *fam83fa*^{F275/279A} mRNA, were resolved by SDS-PAGE and subjected to Western blotting with indicated antibodies.

Figure 2: FAM83F-CK1 α interaction is required for membrane localisation and canonical Wnt signalling effects.

(A) Lysates from U2OS Flp/Trx cells expressing GFP, GFP-FAM83A, GFP-FAM83F, GFP-FAM83F^{C497A}, GFP-FAM83F^{D250A} or GFP-FAM83F^{F284/288A} were subjected to immunoprecipitation with GFP trap beads. Input lysates and GFP IPs were resolved by SDS-PAGE and subjected to Western blotting with the indicated antibodies. **(B)** Representative widefield immunofluorescence microscopy images of U2OS Flp/Trx cells expressing GFP-FAM83F, GFP-FAM83F^{C497A}, GFP-FAM83F^{D250A} or GFP-FAM83F^{F284/288A}, labelled with antibodies recognising GFP (far left panels, green), CK1 α (second row of panels from left, magenta) and DAPI (third row of panels from left, blue). Overlay of GFP, CK1 α and DAPI images as a merge is shown on the right. Immunofluorescence images captured with a 60x objective. Scale bar represents 10 μ m. **(C)** Relative luciferase activity in U2OS Flp/Trx cells expressing GFP, GFP-FAM83F, GFP-FAM83F^{C497A}, GFP-FAM83F^{D250A} or GFP-FAM83F^{F284/288A} treated with either L- or Wnt3A-conditioned medium for 6 h. Luciferase activity is presented as TOPflash luciferase normalised to FOPflash luciferase and Renilla expression, the transfection control plasmid. Data representative of four biological repeats with bar graph representing mean \pm standard

error. Expression of GFP, GFP-FAM83A, GFP-FAM83F, GFP-FAM83F^{C497A}, GFP-FAM83F^{D250A} and GFP-FAM83F^{F284/288A} in U2OS Flp/Trx cells was induced by treatment with 20 ng/ml doxycycline for 24 h. Statistical analysis of (C) was completed using a students unpaired t-test and comparing cell lines as denoted on graph. P-values denoted by asterisks (**** <0.0001, *** <0.001, ** <0.01, * <0.05).

Figure 3: Endogenous FAM83F localises to the plasma membrane and interacts with CK1 α . (A) Extractions from mouse tissues: brain, heart, lung, liver, stomach, small intestine, large intestine, kidney, spleen and intestinal crypts, plus HaCaT wild-type cells were resolved by SDS-PAGE and subjected to Western blotting with indicated antibodies. (B) HCT116 wild-type, HCT116 FAM83F^{-/-} (cl.1), HCT116 FAM83F^{-/-} (cl.2), HCT116 GFP/GFP FAM83F, DLD-1 wild-type, DLD-1 FAM83F^{-/-} and DLD1 GFP/GFP FAM83F cell extracts were resolved by SDS-PAGE and subjected to Western blotting with indicated antibodies. (C) HCT116 wild-type, HCT116 GFP/GFP FAM83F, DLD-1 wild-type and DLD-1 GFP/GFP FAM83F cell extracts were subjected to immunoprecipitation with GFP trap beads. Input lysates and GFP IPs were resolved by SDS-PAGE and subjected to Western blotting with indicated antibodies. (D) HCT116 wild-type, HCT116 FAM83F^{-/-} (cl.1), DLD-1 wild-type and DLD-1 FAM83F^{-/-} cell extracts were subjected to immunoprecipitation with anti-CK1 α antibody. Input lysates and CK1 α IPs were resolved by SDS-PAGE and subjected to Western blotting with indicated antibodies. (E) Representative widefield immunofluorescence microscopy images of HCT116 GFP/GFP FAM83F cells, labelled with antibodies recognising GFP (far left panels, green), CK1 α (second row of panels from left, magenta) and DAPI (third row of panels from left, blue). Overlay of GFP, CK1 α and DAPI images as a merge is shown on the right. Immunofluorescence images captured with a 60x objective. (F) Representative widefield immunofluorescence microscopy images of HCT116 wild-type cells, labelled with antibodies recognising FAM83F (far left panels, green), β -catenin (second row of panels from left, magenta) and DAPI (third row of panels from left, blue). Overlay of FAM83F, β -catenin and DAPI images as a merge is shown on the right. Immunofluorescence images captured with a 100x objective. Scale bar represents 10 μ m.

Figure 4: Knockout of FAM83F reduces canonical Wnt signalling in colorectal cancer cells. (A) qRT-PCR was performed using cDNA from HCT116 wild-type, HCT116 FAM83F^{-/-} (cl.1), HCT116 FAM83F^{-/-} (cl.2), DLD-1 wild-type and DLD-1 FAM83F^{-/-} cells following treatment with L-CM or Wnt3A-CM for 6 h, and primers for *Axin2* and *GAPDH* genes. *Axin2* mRNA expression was normalised to *GAPDH* mRNA expression and represented as fold change compared to L-CM treated wild-type cells. Data represents nine (HCT116 cell lines)

or seven (DLD-1 cell lines) biological repeats with bar graph representing mean \pm standard error. **(B)** HCT116 wild-type, HCT116 FAM83F^{-/-} (cl.1), DLD-1 wild-type and DLD-1 FAM83F^{-/-} cells treated with L-CM or Wnt3A-CM for 6 h, were subjected to immunoprecipitation with CK1 α antibody. Input lysates and CK1 α IPs were resolved by SDS-PAGE and subjected to Western blotting with indicated antibodies. **(C)** Lysates from HCT116 wild-type, HCT116 FAM83F^{-/-} (cl.1), HCT116 FAM83F^{-/-} (cl.2), DLD-1 wild-type and DLD-1 FAM83F^{-/-} cells following treatment with L-CM or Wnt3A-CM for 4 h, were resolved by SDS-PAGE and subjected to Western blotting with indicated antibodies. Statistical analysis of (A) was completed using a students unpaired t-test and comparing cell lines as denoted on graph. P-values denoted by asterisks (**** <0.0001, *** <0.001, ** <0.01, * <0.05).

Figure 5: FAM83F acts up stream of the β -catenin destruction complex. **(A)** qRT-PCR was performed using cDNA from HCT116 wild-type and HCT116 FAM83F^{-/-} (cl.1) cell lines following treatment with L-CM or Wnt3A-CM with or without 5 μ M CHIR99021 for 6 h, and primers for *Axin2* and *GAPDH* genes. *Axin2* mRNA expression was normalised to *GAPDH* mRNA expression and represented as arbitrary units. Data representative of four biological repeats with bar graph representing mean \pm standard error. **(B)** Cytoplasmic, nuclear and membrane lysates from HCT116 wild-type, HCT116 FAM83F^{-/-} (cl.1) and HCT116 FAM83F^{-/-} (cl.2) cell lines were resolved by SDS-PAGE and subjected to Western blotting with indicated antibodies. **(C)** Densitometry of CK1 α protein abundance from (B) membrane lysates normalised to GAPDH protein abundance and represented as fold change compared to HCT116 wild-type cells. Data representative of three biological repeats with bar graph representing mean \pm standard error. **(D)** Cytoplasmic, nuclear and membrane lysates from DLD-1 wild-type and DLD-1 FAM83F^{-/-} cell lines, were resolved by SDS-PAGE and subjected to Western blotting with indicated antibodies. **(E)** Densitometry of CK1 α protein abundance from (D) membrane lysates normalised to Na/K ATPase protein abundance and represented as fold change compared to DLD-1 wild-type cells. Data representative of three biological repeats with bar graph representing mean \pm standard error. Specificity of cytoplasmic, nuclear and membrane compartment lysates from (B) and (D) were determined by Western blotting with subcellular compartment specific antibodies; Alpha-tubulin (cytoplasmic), Lamin A/C (nuclear), U2AF1 (nuclear), Na/K ATPase (membrane). Statistical analysis of (A), (C) and (E) was completed using a students unpaired t-test and comparing cell lines as denoted on graphs. P-values denoted by asterisks (**** <0.0001, *** <0.001, ** <0.01, * <0.05).

Figure 6: Membranous localisation of FAM83F is required for FAM83F's role in canonical Wnt signalling. **(A)** Total cell, cytoplasmic, nuclear and membrane lysates from HCT116 wild-type, HCT116 FAM83F^{WT/C497A} and HCT116 FAM83F^{-/-} (cl.2) cell lines, were resolved by SDS-PAGE and subjected to Western blotting with indicated antibodies. **(B)** Densitometry of FAM83F and CK1 α protein abundance from (A) membrane lysates normalised to GAPDH protein abundance and represented as fold change compared to HCT116 wild-type cells. Data representative of three biological repeats with bar graph representing mean \pm standard error. **(C)** Cell lysates from HCT116 wild-type, HCT116 FAM83F^{-/-} (cl.2) and HCT116 FAM83F^{WT/C497A} cells, were subjected to immunoprecipitation with anti-CK1 α antibody. Input lysates and CK1 α precipitate elutes were resolved by SDS-PAGE and subjected to Western blotting with indicated antibodies. **(D)** qRT-PCR was performed using cDNA from HCT116 wild-type and HCT116 FAM83F^{WT/C497A} cells following treatment with L-CM or Wnt3A-CM for 6 h, and primers for *Axin2* and *GAPDH* genes. *Axin2* mRNA expression was normalised to *GAPDH* mRNA expression and represented as fold change compared to L-CM treated wild-type cells. Data representative of five biological repeats with bar graph representing mean \pm standard error. Statistical analysis of (B) and (D) was completed using a students unpaired t-test and comparing cell lines as denoted on graphs. P-values denoted by asterisks (**** <0.0001, *** <0.001, ** <0.01, * <0.05).

SUPPLEMENTARY FIGURE LEGENDS

Supplementary Figure 1: Canonical Wnt signalling activation following ectopic

expression of GFP-FAM83 proteins. (A) Relative luciferase activity in U2OS Flp/Trx cells expressing GFP-FAM83A, GFP-FAM83B, GFP-FAM83C, GFP-FAM83D, GFP-FAM83E, GFP-FAM83F, GFP-FAM83G, GFP-FAM83H and GFP only treated with either L-CM or Wnt3A-CM for 24 h. TOPflash and FOPflash luciferase activity presented as relative light units normalised to Renilla expression, the transfection control plasmid. Data representative of three biological repeats with bar graph representing mean + standard error. Expression of GFP-FAM83A, GFP-FAM83B, GFP-FAM83C, GFP-FAM83D, GFP-FAM83E, GFP-FAM83F, GFP-FAM83G, GFP-FAM83H and GFP only in U2OS Flp/Trx cells was induced by treatment with 20 ng/ml doxycycline for 24 h.

Supplementary Figure 2: Zebrafish Fam83fa DUF1669 domain and FAM83F

farnesylation mutants can still induce axis duplication. (A) Percentage of *Xenopus* embryos showing phenotypes as depicted in Figure 1A following injection with HA tagged *fam83fa*^{1-555aa(F/L)}, *fam83fa*^{1-500aa}, *fam83fa*^{1-400aa}, *fam83fa*^{1-356aa} or *fam83fa*^{1-300aa (DUF)} mRNA. Data represent three independent experiments with total numbers of embryos observed denoted above the graph. Bar graph represents mean + standard deviation. ****p<0.0001, **p<0.01, two-way ANOVA with Dunnett's post-hoc test to compare the percentage of embryos displaying a wild-type phenotype. **(B)** Protein extracts from *Xenopus* embryos following injection with HA tagged zebrafish *fam83fa*^{1-555aa(F/L)}, *fam83fa*^{1-500aa}, *fam83fa*^{1-400aa}, *fam83fa*^{1-356aa} or *fam83fa*^{1-300aa (DUF)} mRNA were resolved by SDS-PAGE and subjected to western blotting with indicated antibodies. **(C)** Percentage of *Xenopus* embryos showing phenotypes as depicted in Figure 1A following injection with human FAM83F or FAM83F^{C497A} mRNA. Data represent one independent experiment with total numbers of embryos denoted above the graph. n.s = not significant, Chi squared test. F/L = full-length. DUF = Domain of unknown function 1669.

Supplementary Figure 3: FAM83F is identified as farnesylated by mass spectrometry.

(A) HEK293 Flp/Trx cells expressing GFP-FAM83F were lysed and subjected to immunoprecipitation with GFP trap beads. GFP eluted proteins were resolved by SDS-PAGE, protein bands were excised and trypsin-digested for mass spectrometry analysis. Mass spectrometry peptide coverage of the FAM83F protein sequence as demonstrated by highlighted residues. **(B)** Two detected peptides which correspond to the C'-terminal residues of FAM83F protein with both non-farnesylated peptides and farnesylated peptides identified by mass spectrometry. **(C)** Fragmentation of the farnesylated peptide to confirm

presence of a farnesyl group on the cysteine residue which corresponds to the CAAX box cysteine.

Supplementary Figure 4: FAM83F expression in various cell lines. (A) Cell lysates from A-172, A549, NMuMG, SK-OV-3, K-562, MDA-MB-468, U2OS, PC-3, ARPE-19, SH-SY5Y, HUH7, THP-1 and HCT116 cells were resolved by SDS-PAGE and subjected to Western blotting with indicated antibodies. **(B)** Table indicating the cell of origin for all the cell lines used in (A).

Supplementary Figure 5: Sequencing of CRISPR/Cas9 cell lines. (A) DNA sequence of *FAM83F* exon 2 for HCT116 wild-type and HCT116 *FAM83F*^{-/-} (cl.1) cell lines indicating large deletion in *FAM83F* exon 2 in HCT116 *FAM83F*^{-/-} (cl.1) cell lines. **(B)** Expected DNA sequence and actual DNA sequence of HCT116 ^{GFP/GFP}*FAM83F* cell lines of the transition zone between *GFP* and *FAM83F* exon 1.

Supplementary Figure 6: Negative controls for anti-FAM83F antibody

immunofluorescence. (A) Representative widefield immunofluorescence microscopy images of HaCaT wild-type cells and HaCaT *FAM83F*^{-/-} cells, labelled with antibodies recognising FAM83F (far left panels, green), F-actin (second row of panels from left, magenta) and DAPI (third row of panels from left, blue). Overlay of FAM83F, F-actin and DAPI images as a merge is shown on the right. Immunofluorescence images captured with a 20x objective. Scale bar represents 10 µm

Supplementary Figure 7: FAM83F knockout reduces canonical Wnt signalling in non-colorectal cancer cell lines. (A)

Cell lysates from U2OS wild-type and U2OS *FAM83F*^{-/-} cells were subjected to immunoprecipitation with anti-FAM83F antibody. FAM83F IPs were resolved by SDS-PAGE and subjected to Western blotting with FAM83F antibody. **(B)** Relative luciferase activity in U2OS wild-type and U2OS *FAM83F*^{-/-} cells treated with either L-CM or Wnt3A-CM for 6 h. Luciferase activity presented as TOPflash luciferase normalised to FOPflash luciferase and Renilla expression, the transfection control plasmid. Data representative of three biological repeats with bar graph representing mean ± standard error. **(C)** qRT-PCR was performed using cDNA from U2OS wild-type and U2OS *FAM83F*^{-/-} cell lines following treatment with L-CM or Wnt3A-CM with or without 5 µM CHIR99021 for 6 h, and primers for *Axin2* and *GAPDH* genes. *Axin2* mRNA expression was normalised to *GAPDH* mRNA expression and represented as fold change compared to L-CM treated cells. Data representative of six biological repeats with bar graph representing mean ± standard error. Statistical analysis of (B) and (C) was completed using a students unpaired t-test and

comparing cell lines as denoted on graphs. P-values denoted by asterisks (**** <0.0001, *** <0.001, ** <0.01, * <0.05).

SUPPLEMENTARY MATERIALS AND METHODS

Mass spectrometry

Mass spectrometry was performed as previously described (1). Briefly, expression of GFP-FAM83F in HEK293 Flp/Trx cells was induced with doxycycline 24 h prior to lysis. Cells were lysed and proteins were immunoprecipitated using GFP-Trap Agrose beads (Chromotek) as described in main methods section. Proteins were separated by 4-12% gradient SDS-PAGE, stained with InstantBlue and gel slices covering each lane were excised and trypsin-digested. Mass spectrometry analysis of the peptides was performed by LC-MS/MS on the Linear Ion Trap-Orbitrap Hybris Mass Spectrometer (Orbitrap Velos Pro, Thermo Fisher Scientific) coupled to a U3000 RSLC Hplc (Thermo Fisher Scientific). Peptides were trapped on a nanoViper Trap column and (2 cm x 100 μ m, C18, 5 μ m, 100 Å; Thermo Fisher Scientific) and then separated on a 15 cm EASY-spray column (ES800, Thermo Fisher Scientific) equilibrated with a flow of 300 nl/ml of 3% solvent B[80% acetonitrile, 0.08% formic acid, 3% DMSO in H₂O]. The following elution gradient was completed: time (min)/solvent B (%) [0:3, 5:3, 45:35, 47:99, 52:99, 55:3, 60:3]. Data were acquired in the data-dependent mode, automatically switching between MS and MS/MS acquisition. Full-scan spectra [mass/charge ratio (m/z) = 400-1600] were acquired in the Orbitrap with resolution $R=60,000$ at m/z 400 (after accumulation to a Fourier Transform Mass Spectrometry (FTMS) Full Automatic Gain Control (AGC) Target value of 1,000,000 and an FTMS Msn AGC Target value of 50,000). The 20 most intense ions, above a specified minimum signal threshold (2000), based on a low-resolution ($R=15,000$) preview of the survey scan, were fragmented by collision-induced dissociation and recorded in the linear ion trap (Full AGC Target, 30,000; Msn AGC Target, 50000). Data files were analysed by Proteome Discoverer 2.0 (www.thermoscientific.com), using Mascot 2.4.1 (www.matrixscience.com) and the SwissProt Human database. Mascot result files were examined using Scaffold Q/Q+S V4.4.7 (www.proteomesoftware.com). Allowance was made for the following fixed [carbamidomethyl (C)] and variable modifications [oxidation (M) and deoxidation (M)]. Error tolerances were 10 parts per million for MS1 and 0.6 Da for MS2.

Figure 1: Fam83f induces axis duplication in *Xenopus* embryos through an interaction with CK1 α

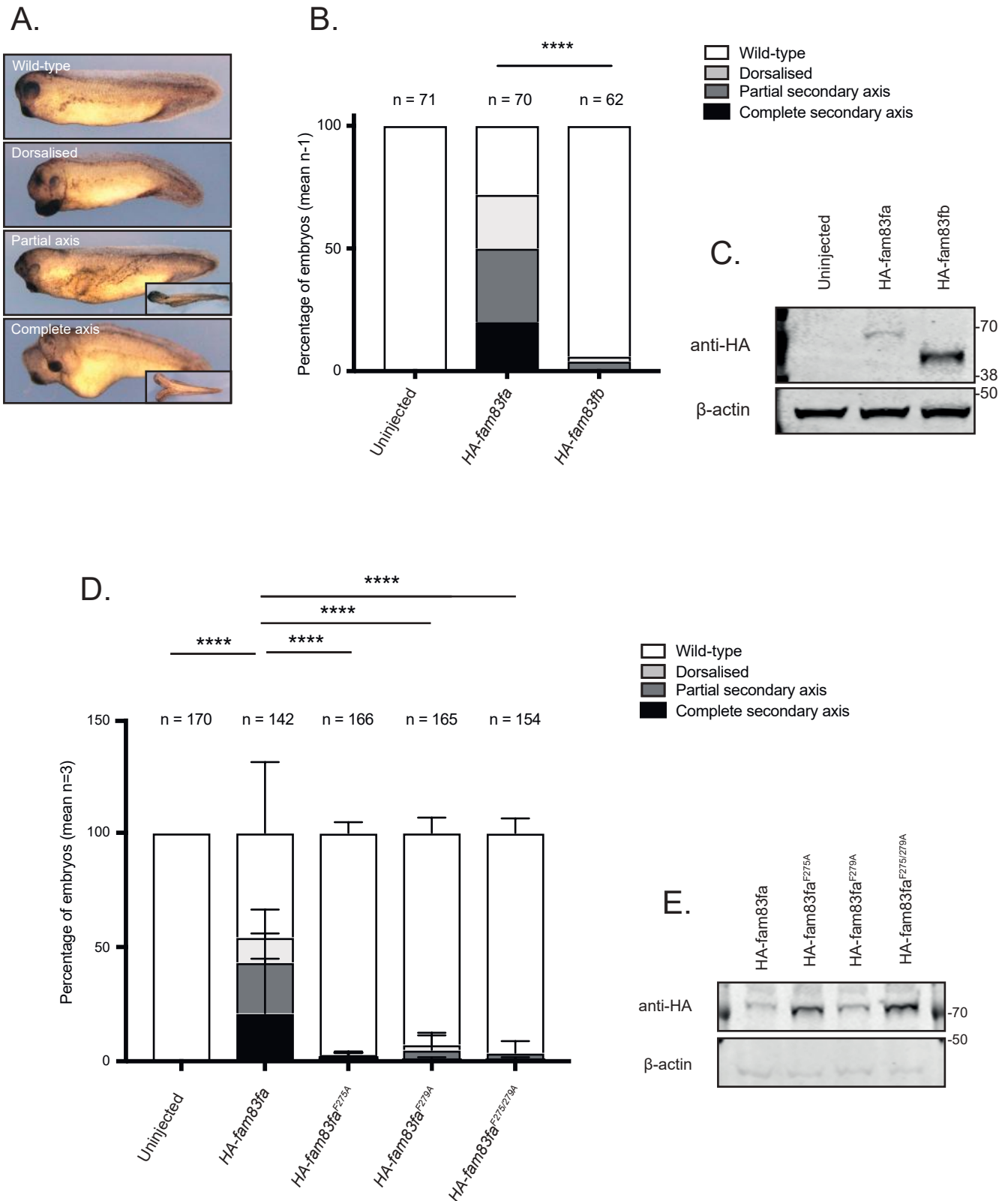


Figure 2: FAM83F-CK1 α interaction is required for membrane localisation and canonical Wnt signalling effects

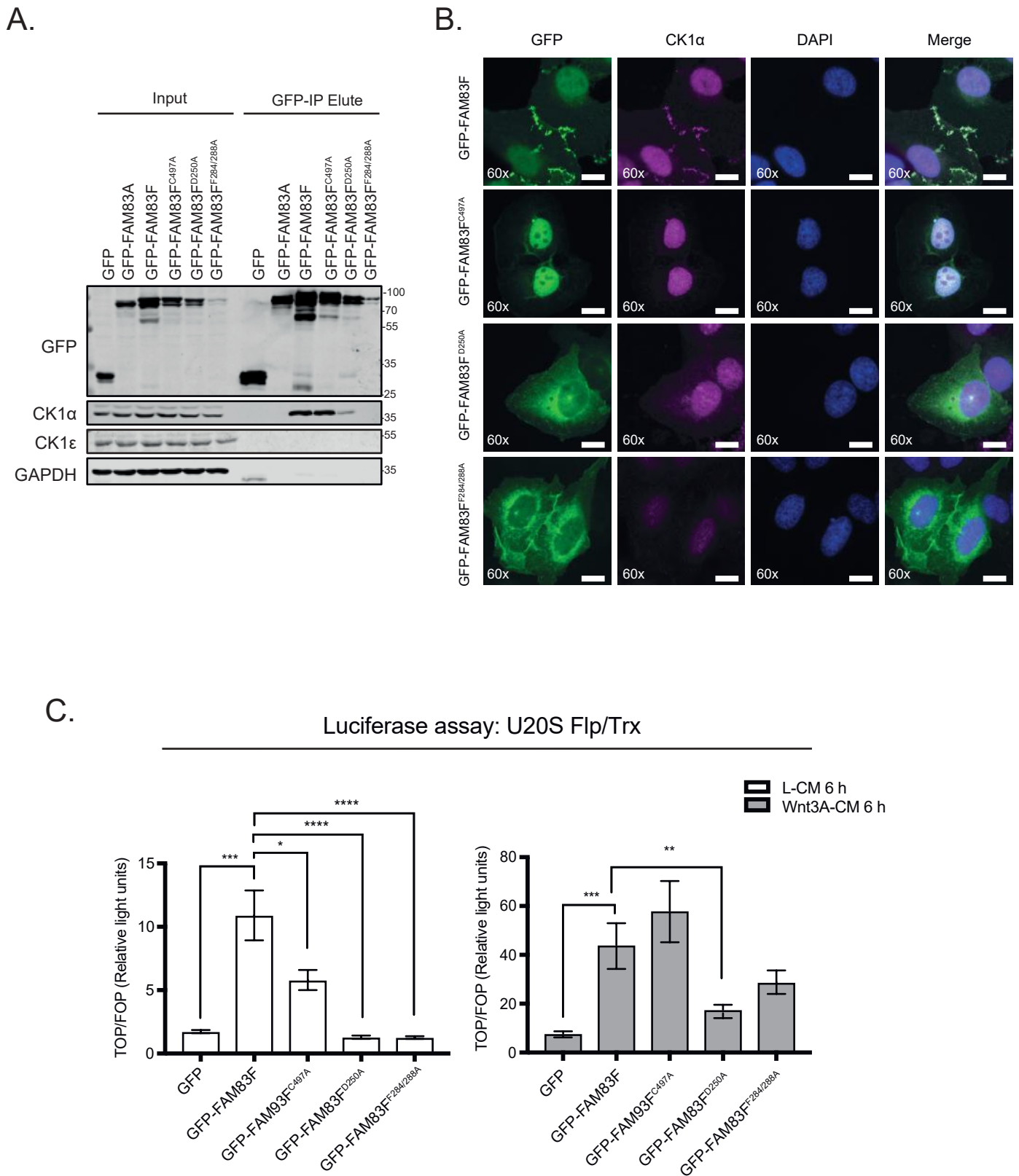


Figure 3: Endogenous FAM83F localises to plasma membrane and interacts with CK1 α

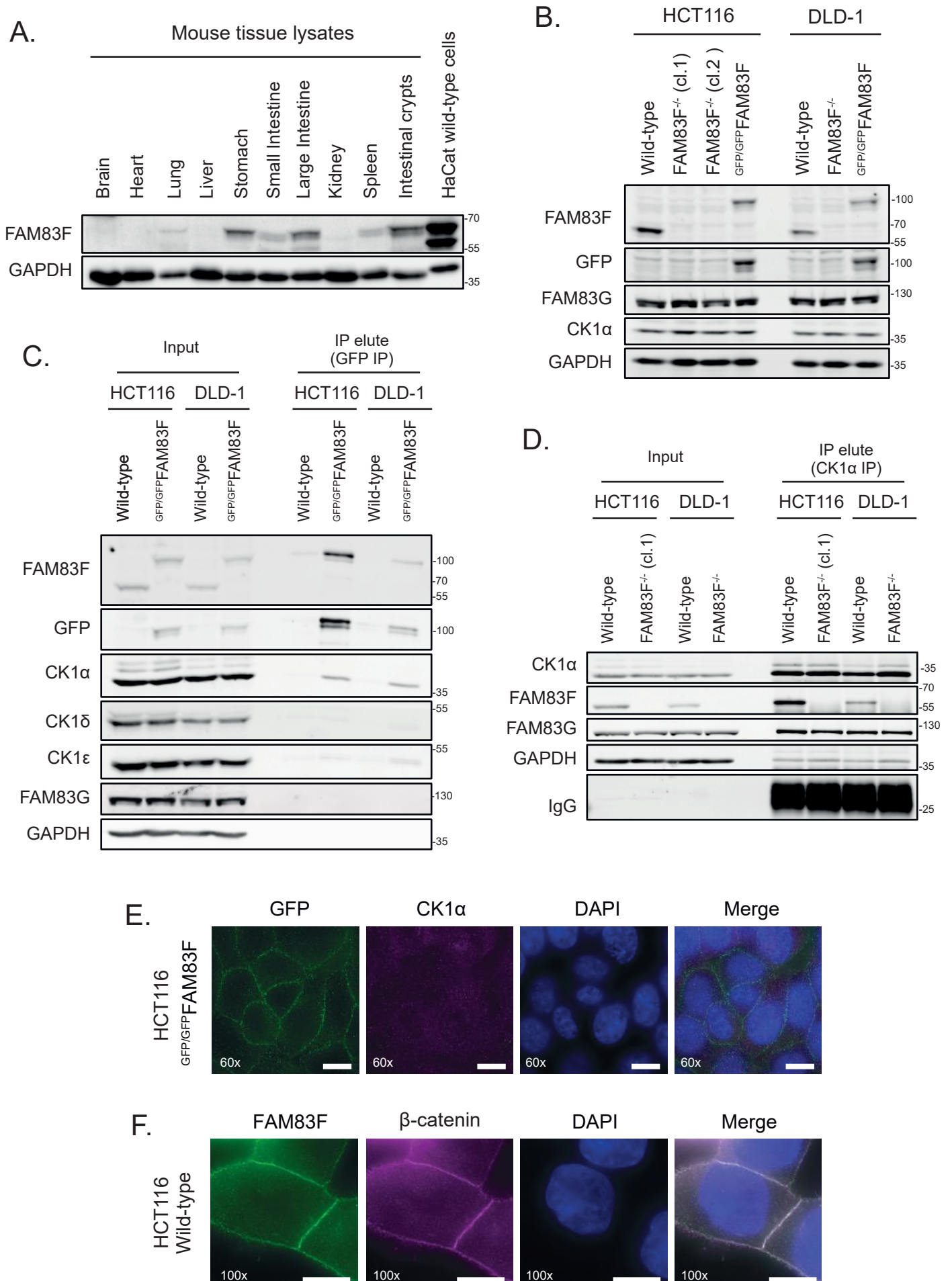


Figure 4: Knockout of FAM83F reduces canonical Wnt signalling in colorectal cancer cells

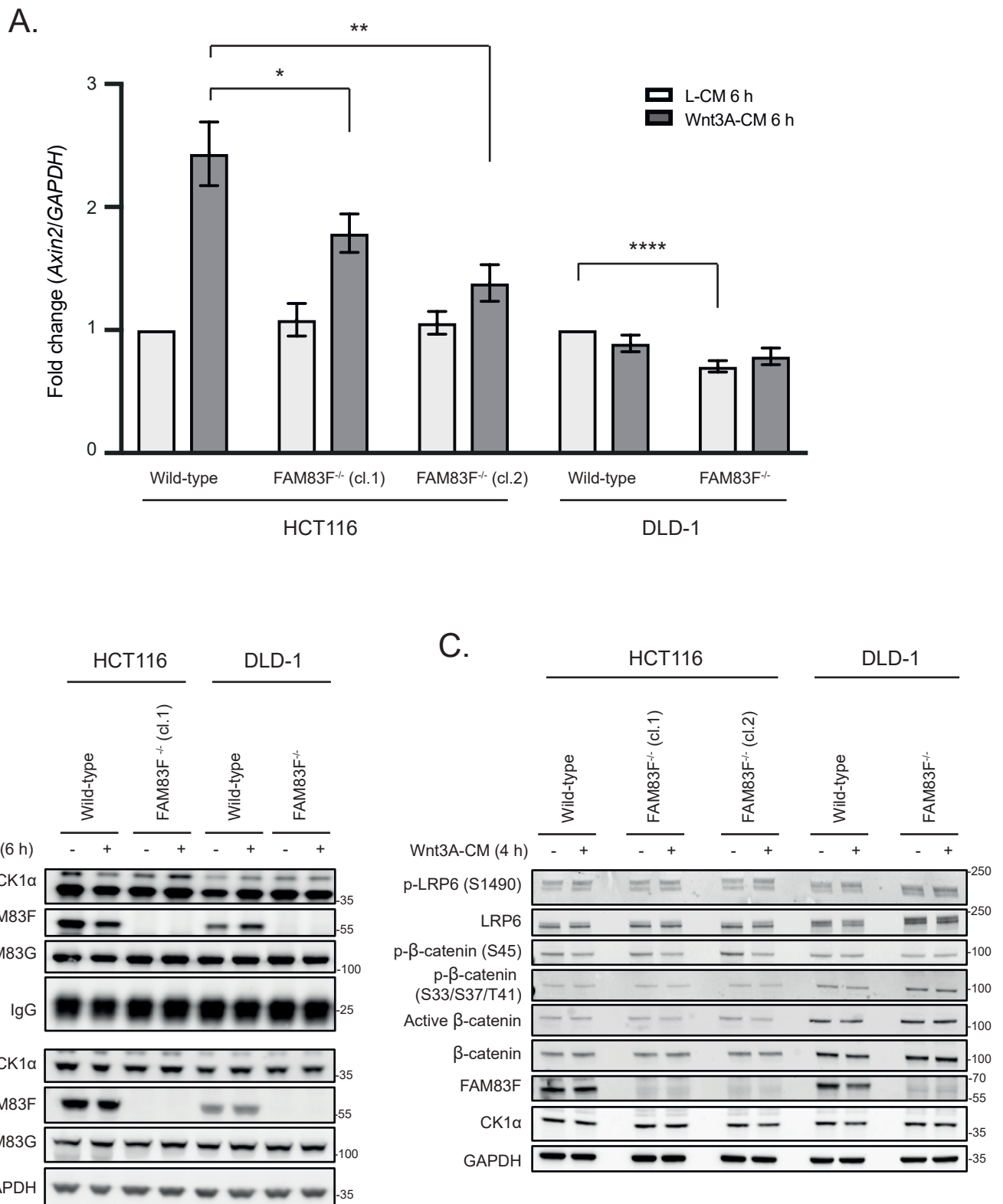


Figure 5: FAM83F acts upstream of the β -catenin destruction complex

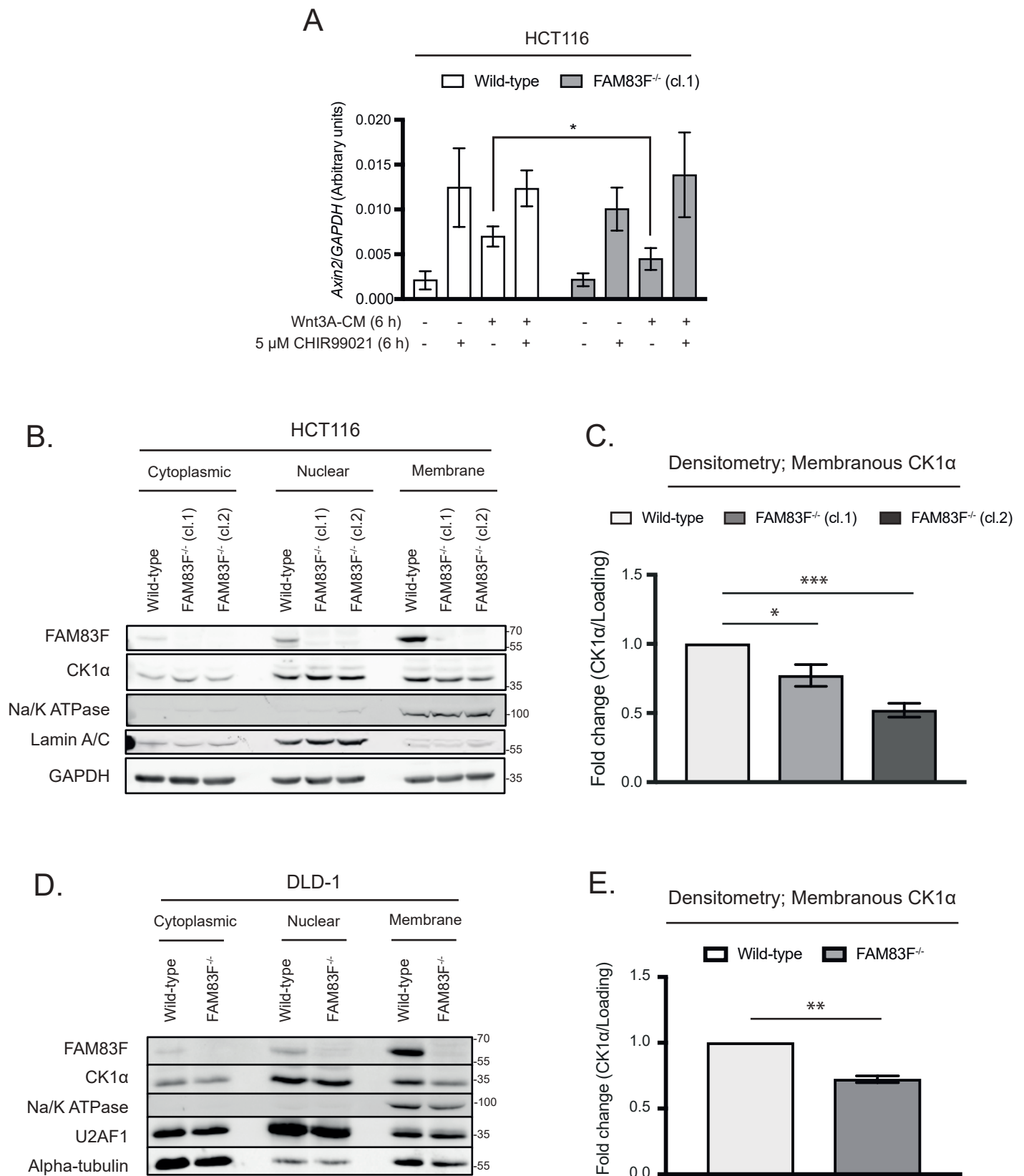
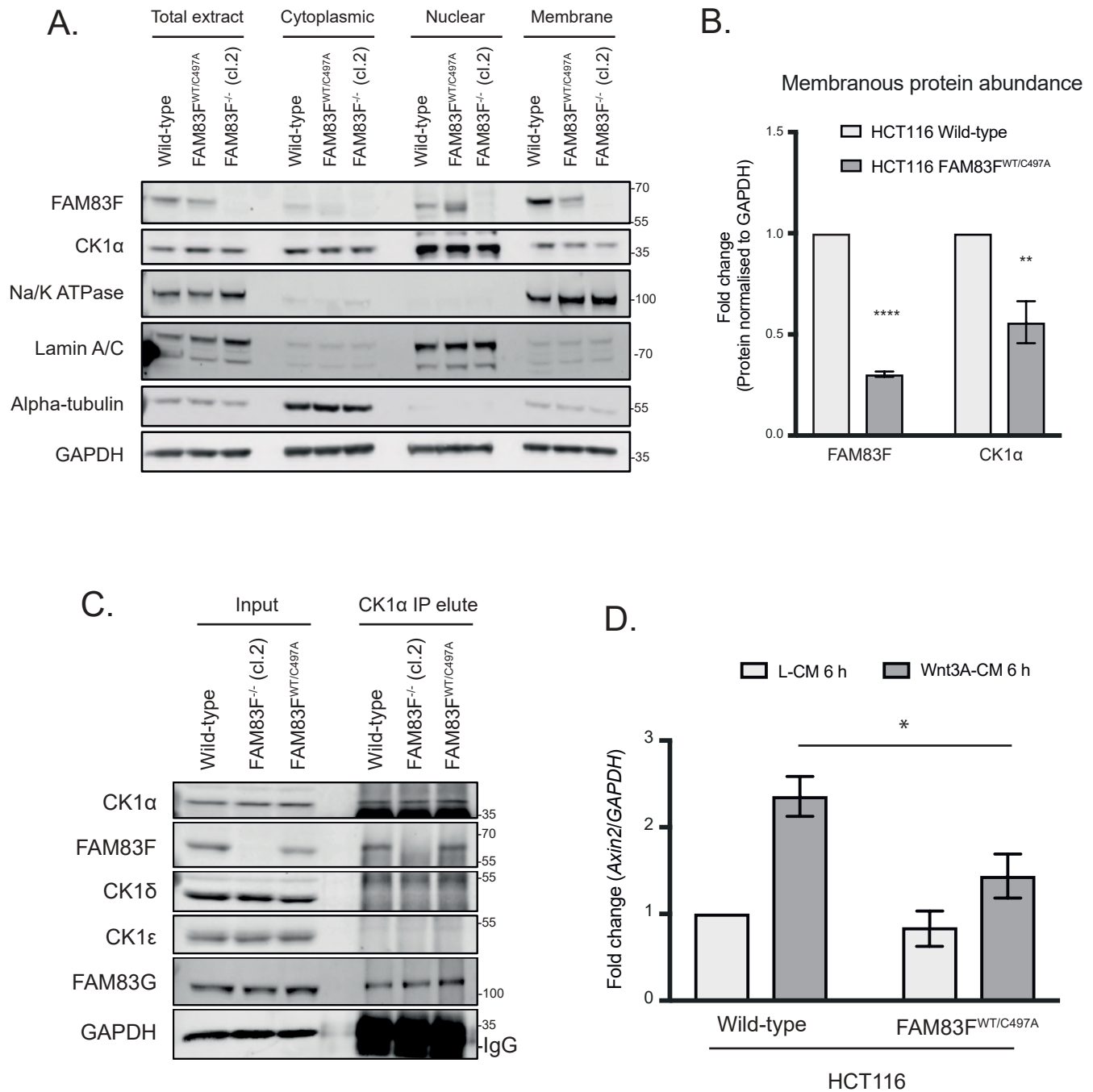


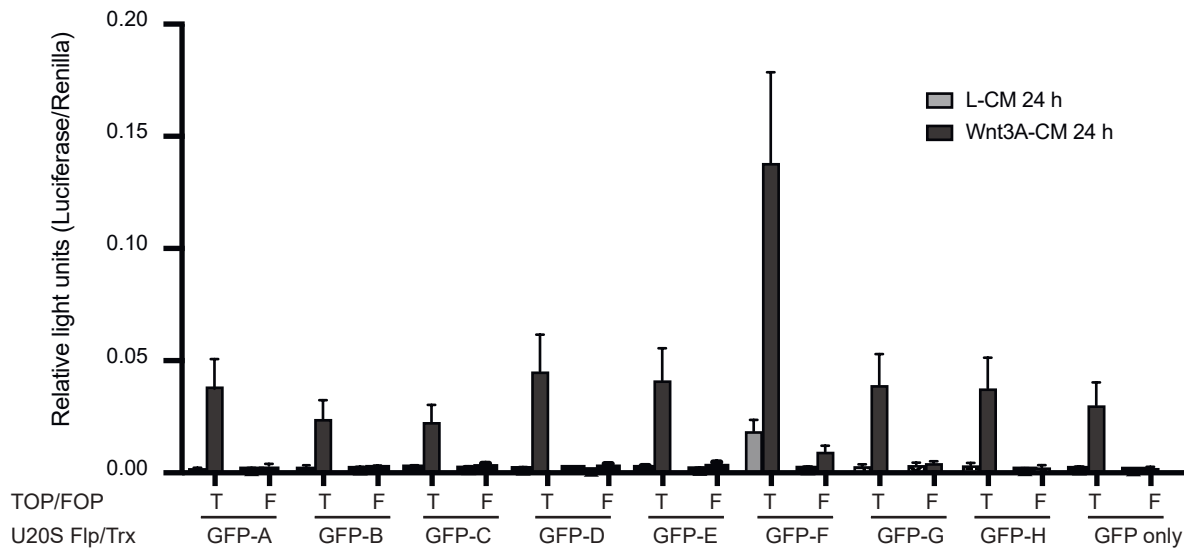
Figure 6: Membranous localisation of FAM83F is required for FAM83F's role in canonical Wnt signalling



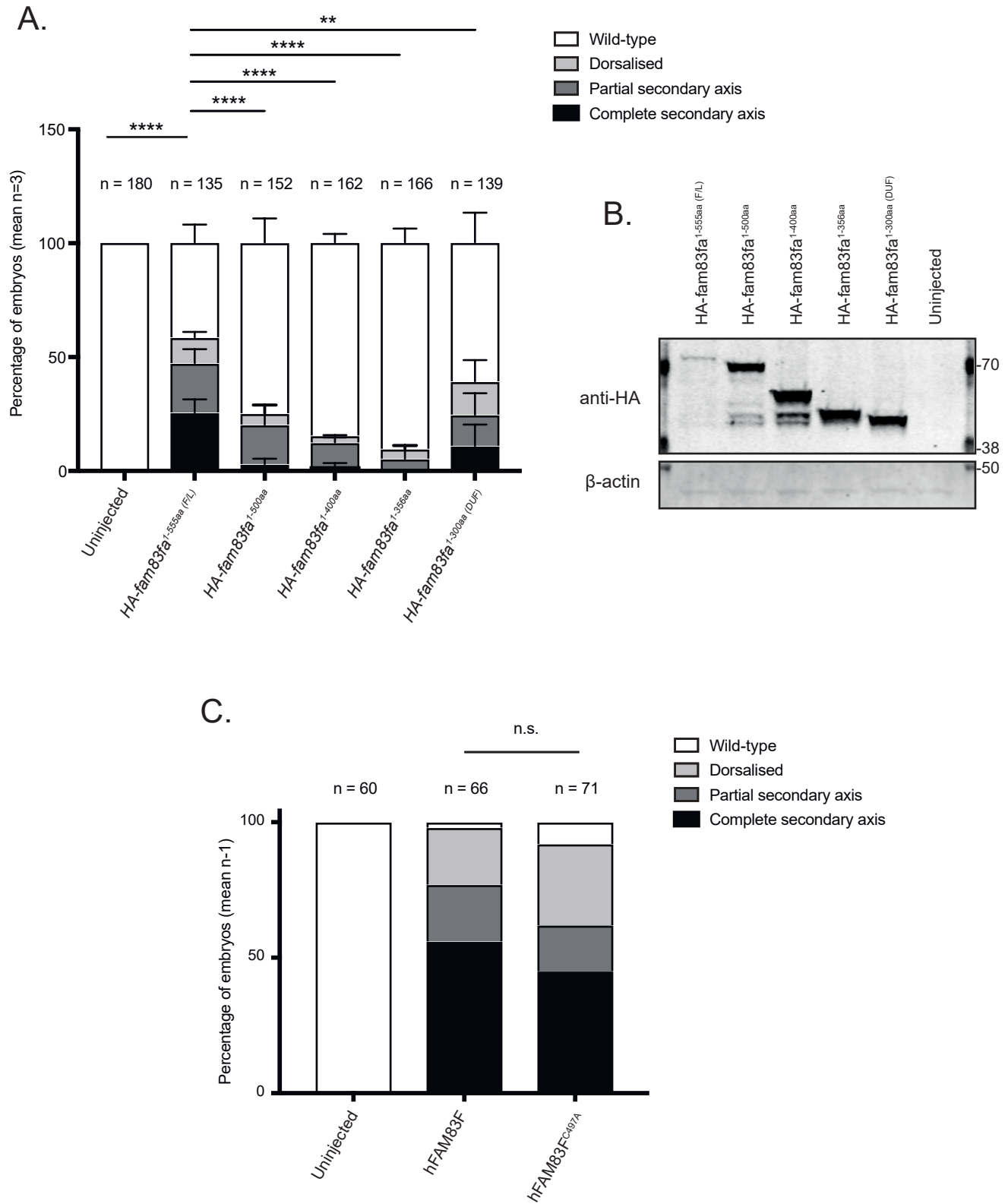
Supplementary Figure 1: Canonical Wnt signalling activation following ectopic expression of GFP-FAM83 proteins

A.

Luciferase assay: U20S Flp/Trx GFP-FAM83 proteins



Supplementary Figure 2: Zebrafish Fam83fa DUF1669 domain and FAM83F farnesylation mutants can still induce axis duplication



Supplementary Figure 3: FAM83F is identified as farnesylated by mass spectrometry

A.

FAM83F_HUMAN (100%), 55,486.3 Da
 Protein FAM83F OS=Homo sapiens GN=FAM83F PE=1 SV=1
 53 exclusive unique peptides, 101 exclusive unique spectra, 1433 total spectra, 444/600 amino acids (89% coverage)

M	A	E	S	Q	L	N	C	L	D	E	A	H	V	N	E	K	V	T	E	A	Q	A	A	F	Y	C	E	R	R	R	A	A	L	E	A	L	L	G	G	G	E	Q	A	Y	R	R	E	L	K	E	E	Q	L	R	D	F	L	S	S	P	E	R	Q	A	L	R	A	A	W	S	P	Y	E	D	A	V	P	A	
A	N	A	R	G	K	S	K	A	K	A	K	A	P	A	P	A	P	A	E	S	G	E	S	L	A	Y	W	P	D	R	S	D	T	E	V	P	P	L	D	L	G	W	T	D	T	G	F	Y	R	G	V	S	R	V	T	L	F	T	H	K	Q	V	V	R	Q	M	I	Q	Q										
A	Q	K	V	I	A	V	M	D	L	F	T	D	G	I	F	Q	D	I	V	D	A	A	C	K	R	R	V	P	V	Y	I	I	L	D	E	A	G	V	K	Y	F	L	E	M	C	Q	D	L	Q	L	T	D	F	R	I	R	N	I	R	V	R	S	V	T	G	V	G	F	Y	M	P	M	G	R	I	K	G		
T	L	S	S	R	F	L	M	V	D	G	D	K	V	A	T	G	S	Y	R	F	T	W	S	S	S	H	V	D	R	N	L	L	L	L	L	T	G	Q	N	V	E	P	F	D	T	E	F	R	E	L	Y	A	I	S	E	E	V	D	L	Y	R	Q	L	S	L	A	G	R	V	G	L	H	Y	S	S	T	V	A	R
K	L	I	N	P	K	Y	A	L	V	S	G	C	R	H	P	P	G	E	M	M	R	W	A	A	R	Q	Q	R	E	A	A	G	N	P	E	G	Q	E	E	G	A	S	G	G	E	S	A	W	R	L	E	S	F	L	K	D	L	V	T	V	E	Q	V	L	P	P	V	E	P	I	P	L	G	E	L	S	Q	K	D
G	R	M	V	S	H	M	H	R	D	L	K	P	K	S	R	E	A	P	S	R	N	G	M	G	E	A	A	R	G	E	A	A	P	A	R	R	F	F	S	R	L	F	S	R	R	A	K	R	P	A	A	P	N	G	M	A	S	S	V	S	T	E	T	S	E	V	E	F	L	T	G	K	R	P	N	E	N	S	S
A	D	I	S	G	K	T	S	P	S	S	A	K	P	S	N	C	V	I	S																																																												

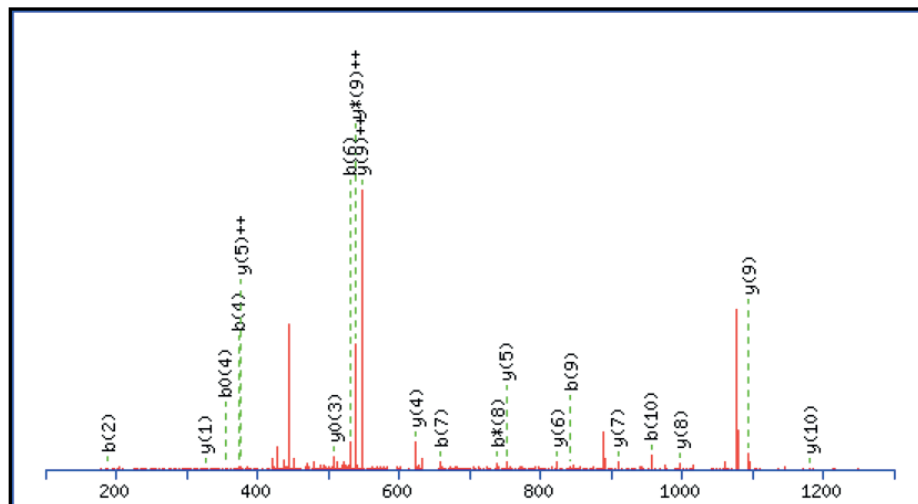
B.

Detected Peptides

Obs. Mass	Calc.mass	Score	Peptide
568.2557	1134.4975	62	K.TSPSSAKPSNC.V
641.8386	1281.6639	42	K.TSPSSAKPSNC.V + Farnesyl

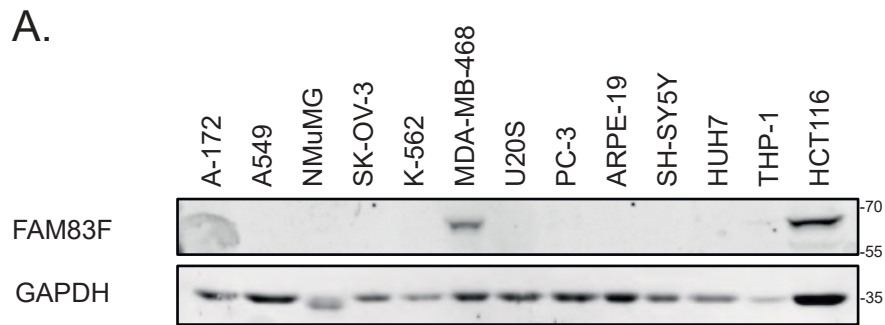
C.

Fragmentation of 1281.6639 peptide confirms farnesylation at cysteine 11



#	b	b ⁺⁺	b [*]	b ⁺⁺⁺	b ⁰	b ⁰⁺⁺	Seq.	y	y ⁺⁺	y [*]	y ⁺⁺⁺	y ⁰	y ⁰⁺⁺	#
1	102.0550	51.5311			84.0444	42.5258	T							11
2	189.0870	95.0471			171.0764	86.0418	S	1181.6235	591.3154	1164.5969	582.8021	1163.6129	582.3101	10
3	286.1397	143.5735			268.1292	134.5682	P	1094.5914	547.7994	1077.5649	539.2861	1076.5809	538.7941	9
4	373.1718	187.0895			355.1612	178.0842	S	997.5387	499.2730	980.5121	490.7597	979.5281	490.2677	8
5	460.2038	230.6055			442.1932	221.6003	S	910.5067	455.7570	893.4801	447.2437	892.4961	446.7517	7
6	531.2409	266.1241			513.2304	257.1188	A	823.4746	412.2409	806.4481	403.7277	805.4641	403.2357	6
7	659.3359	330.1716	642.3093	321.6583	641.3253	321.1663	K	752.4375	376.7224	735.4110	368.2091	734.4269	367.7171	5
8	756.3886	378.6980	739.3621	370.1847	738.3781	369.6927	P	624.3425	312.6749	607.3160	304.1616	606.3320	303.6696	4
9	843.4207	422.2140	826.3941	413.7007	825.4101	413.2087	S	527.2898	264.1485	510.2632	255.6353	509.2792	255.1432	3
10	957.4636	479.2354	940.4370	470.7222	939.4530	470.2302	N	440.2578	220.6325	423.2312	212.1192			2
11							C	326.2148	163.6111					1

Supplementary Figure 4: FAM83F expression in various cell lines



B.

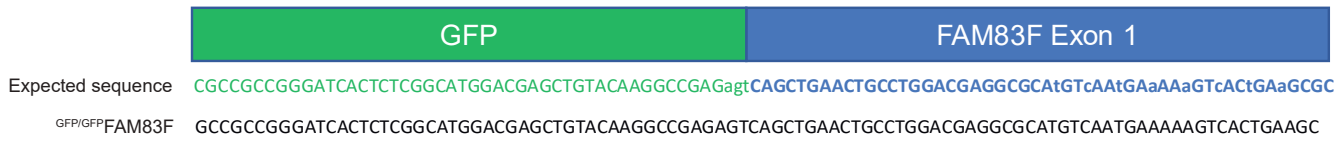
Cell line	Origin
A-172	Glioblastoma
A549	Lung carcinoma
NMuMG	Mouse Mammary epithelium
SK-OV-3	Ovarian Adenocarcinoma
K-562	Chronic Myelogenous Leukemia
MDA-MB-468	Mammary Adenocarcinoma
U20S	Osteosarcoma
PC-3	Prostate epithelium
ARPE-19	Retinal pigment epithelium
SH-SY5Y	Neuroblastoma
HUH7	Hepatocyte derived epithelium
THP-1	Acute Monocytic Leukemia
HCT116	Colorectal cancer

Supplementary Figure 5: Sequencing of CRISPR/Cas9 cell lines

A.

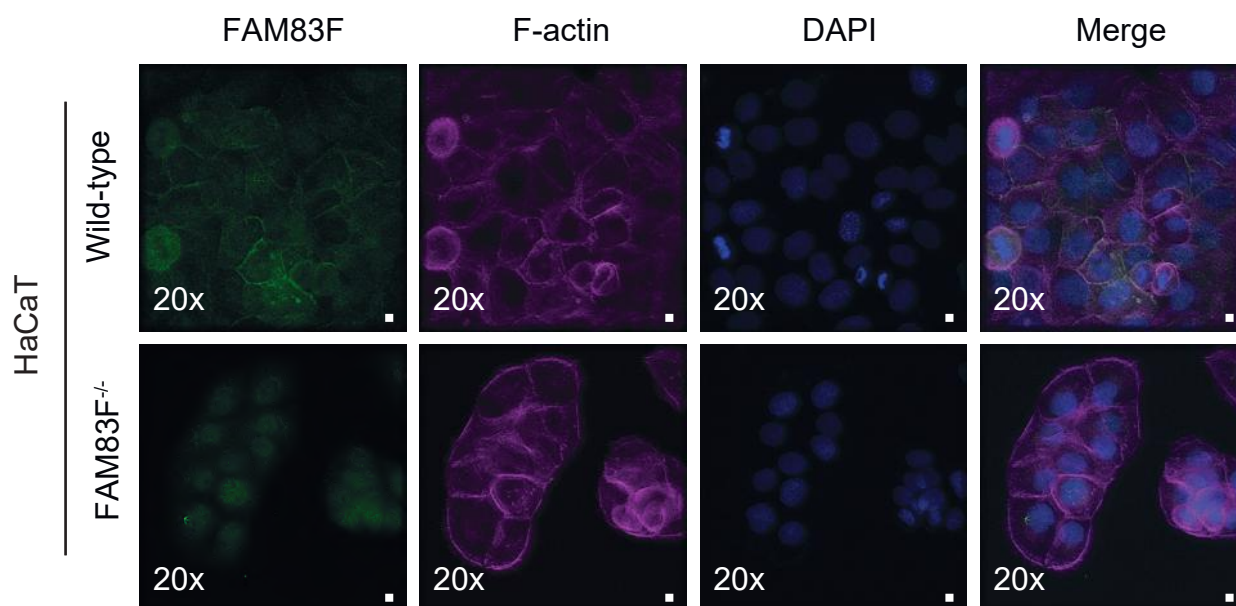


B.



Supplementary Figure 6: Immunofluorescence negative controls for FAM83F antibody

A.



Supplementary Figure 7: FAM83F knockout reduces canonical Wnt signalling in non-colorectal cancer cell lines

